SLIM DESIGN OF POWER SUPPLY UNIT FOR OLED TV BY USING HALF BRIDGE LLC RESONANT CONVERTER TOPOLOGY

A Thesis

by

Samet KURT

Submitted to the
Graduate School of Sciences and Engineering
In Partial Fulfillment of the Requirements for
the Degree of

Master of Science

in the
Department of Electrical and Electronics Engineering

Özyeğin University
June 2021

SLIM DESIGN OF POWER SUPPLY UNIT FOR OLED TV BY USING HALF BRIDGE LLC RESONANT CONVERTER TOPOLOGY

Approved by:

Asst. Prof. Göktürk Poyrazoğlu, Advisor
Department of Electrical and Electronics Engineering
Özyeğin University

Asst. Prof. Kadir Durak
Department of Electrical and Electronics Engineering
Özyeğin University

Asst. Prof. Abdül Balıkcı
Department of Electrical and Electronics Engineering
Dokuz Eylül University

Date Approved: 9 June 2021

To my wife, my family and memory of my grandmother

ABSTRACT

Recently, with the development of technology, televisions which have with different structures and features have been developed in the field of TV. Tv technologies such as QLED, Miniled and OLED, which are developed as rivals to traditional LED TVs, continue to become widespread in the market everyday. OLED TVs do not have a backlight structure, and each pixel is radiated by itself, it enables a thinner design. Since each pixel is spontaneously luminous, it provides good picture quality and allows to see blacks more black and colors more clearly. OLED TV panels are generally supplied in the 20-28V voltage range. The higher power consumption is required with higher luminance and nits values increasing everyday. Power cards have certain mechanical limitations in design, such as thin TV design and limit of specific area. As a result, there is a need for a high efficiency card design that can operate reliably at high currents. The power supply is designed under three main blocks that is EMI filter and rectifier stage, interleaved PFC stage, half-bridge LLC coverter stage. Filter block structure is as C-L-C-L-C. An interleaved PFC block which has 390V output voltage is designed to transfer high power. For the PFC stage, the efficiency is aimed at %95.Temperature comparison has been made with different transformer types on the half-bridge LLC resonant converter. The advantages and disadvantages of using EFD and toroidal cores have been determined. EFD type core is an integrated transformer. When using toroidal transformer, extra series resonant coil is used to dissipate the heating. In this way, high power is transfered with toroidal transformer. Synchronous rectifier is used on the secondary side to increase efficiency . LLC resonant converter stage efficiency is aimed at %96. For the power supply, input voltage range is between 100VAC-270VAC and output power is 384W in 24V@16A.

ÖZETÇE

Son zamanlarda teknolojinin gelişmesiyle birlikte TV alanında da farklı yapı ve özelliklere sahip televizyonlar geliştirildi. Geleneksel LED TV'lere ek olarak geliştirilen QLED, Miniled ve OLED gibi teknolojiler piyasada günden güne yaygınlaşmaya devam ediyor. OLED TV'lerin backlight yapısı olmayıp her bir piksel kendiliğinden ışıdığı için daha ince yapıda tasarım yapılmasını sağlıyor. Her bir piksel kendiliğinden ışıdığı için iyi resim kalitesi sunar ve siyahları daha siyah renkleri daha net görebilme imkanı sunar. OLED TV panelleri genel olarak 20-28V voltaj aralığında beslenirler. Günden güne artan yüksek lüminans ve nits değerleri ile daha yüksek güç tüketimlerine ihtiyaç duyulur. İnce TV tasarımı, belirli alana girebilme sınırı ile güç kartları yüksek akımda güvenilir calışabilen ve yüksek verimlilikteki kart tasarımı ihtiyacı duyulur. Yukarıdaki parametreler düşünülerek tasarlanan güç kartında EMI filtre bloğu, interleaved PFC stage, half-bridge LLC coverter stage olmak üzere üç ana blok altında tasarlanmıştır. EMI filtre bloğu C-L-C-L-C yapıda filtre bloğu kullanılmıştır. Yüksek güçlere çıkabilmek için 390V çıkış gerilimine sahip interleaved PFC bloğu tasarlanmıştır. PFC stage için verim %95 olarak hedeflenmiştir. Half bridge LLC converter üzerinde farklı transformatör tipleri ile sıcaklık karşılaştırma yapılmıştır. EFD ve toroidal core'lar kullanarak avantaj ve dezavantajları belirlenmiştir. LLC converterda geleneksel transformatör yapısından farklı olarak ana transformatör ve kacak enduktans ayrılarak daha yüksek güc transferleri yapılmıştır. Verimi artırmak için sekonder tarafta senkron rectifier kullanılmıştır. LLC resonant converter stage verimi %96 olarak hedeflenmiştir. Güç kartı için, giriş voltaj aralığı 100VAC-270VAC arasında ve çıkış gücü 24V @16A'da 384W'dır.

ACKNOWLEDGEMENTS

Firstly, I would like to thank my advisor Asst. Prof. Gokturk Poyrazoğlu for his assist, suggestion and support during all thesis study. His feedbacks, comments and knowledge are very precious for me and my future.

I am grateful to my managers who are Osman Oral Kıvrak and Cengiz Tarhan. Their theoretical and practical knowledge guided me during all working time. I would like to thank also my colleagues for their valuable supports in Vestel Power Electronic R&D Group.

Finally, I would like to thank especially my wife Şule Nur Baş Kurt and my parents for their encouragement and patience.

TABLE OF CONTENTS

LIST OF TABLES

LIST OF FIGURES

CHAPTER I

INTRODUCTION

1.1 Motivation

In television(TV) technology, there is an increase in luminance values with new trend technologies. Increasing power consumption causes power transfer that has high efficiency in a specific area. High power requirement, even in small size televisions(TV), causes the power supply design which is in certain sizes. New technologies such as organic led-emitting diode(OLED), Quantum Dot, Mini led have some features that are high luminance, high contrast ratio, and brighter color tones. High resolutions are offered to the audience with 8K technology. High Luminous Efficacy (lm/W) values are possible by high power consumption or improving different optical structures [1].

In mini-led TV technology, there are many small-sized light-emitting diodes(LED) on the back-light. Small LEDs are divided into certain groups which are called zones. Each zone is controlled differently, and increase the contrast ratio [2]. In Quantum Dot TVs, an extra film is added between the panel and the backlight[3]. It is the technology that enables colors to be seen brighter [3].The light is emitted in each pixel, which has its own color pigments. Each color is brighter, blacks are more black, and have a higher contrast ratio[4].

1.2 History of TVs

The first television was invented by John Logie Baird in England in the 1920s[5]. Television started to be used more widely with the invention of color televisions in the following years. Fig.1 represent the classification of TV technologies.

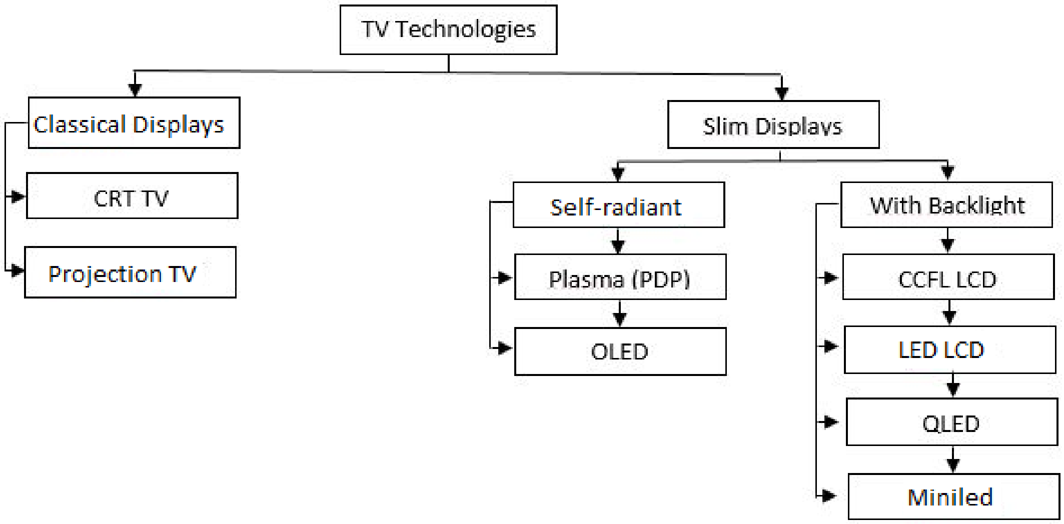

Figure 1: Classification of TV technologies

CRT (Cathode Ray Tube) televisions generate light with electron guns. Electrons that come from a heated cathode tube, hit the phosphor surface on the TV screen and the light occurs on the screen[6]. CRT TVs feature a high contrast ratio, fast pixel response, and bright colors. Disadvantages are heavy, image geometry may be distorted and has low resolution.

Projection TVs offer the opportunity to watch TV on a larger screen. The main control is provided with a DLP control board inside the TV. The image is reflected on the screen with a strong light source and a projection lens. Its biggest advantage is that it can be viewed on a much larger screen. However, it must be viewed from a certain angle to see the image clearly[7]. Low contrast ratio, low resolution are disadvantages for projection TVs[7].

In Plasma TVs, all pixels are arranged in a matrix structure. There are 3 different electrodes in each pixel, which are red, green, and blue as shown in Fig.2.

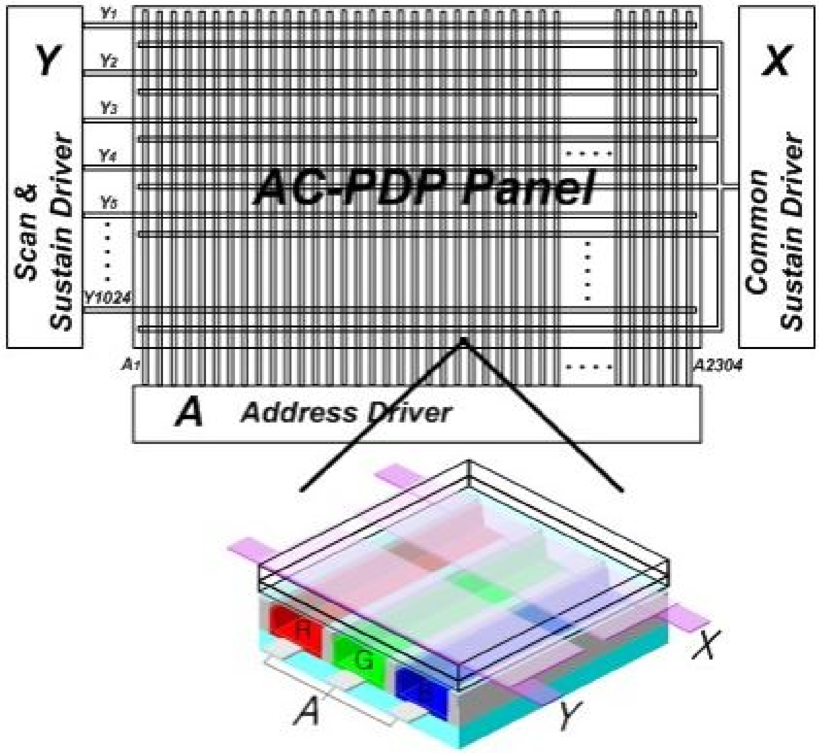

Figure 2: Electrode configuration of plasma TV[8]

Each pixel has small gas plasma cells. these cells emit light with electrical energy. With the Plasma technology, an image was obtained with a thinner screen. It has a high contrast ratio, high resolution, bright picture features. One of the biggest disadvantages is that when the image stays in a certain place for a long time, the blackness may occur in this area[8]. Plasma TVs have high power consumption[8]. High temperature occurs inside the TVs[8].

LCD (Liquid Crystal Display) TV consists of many pixels filled with liquid crystals. The detailed structure of LCD TV is demonstrated in Fig.3.

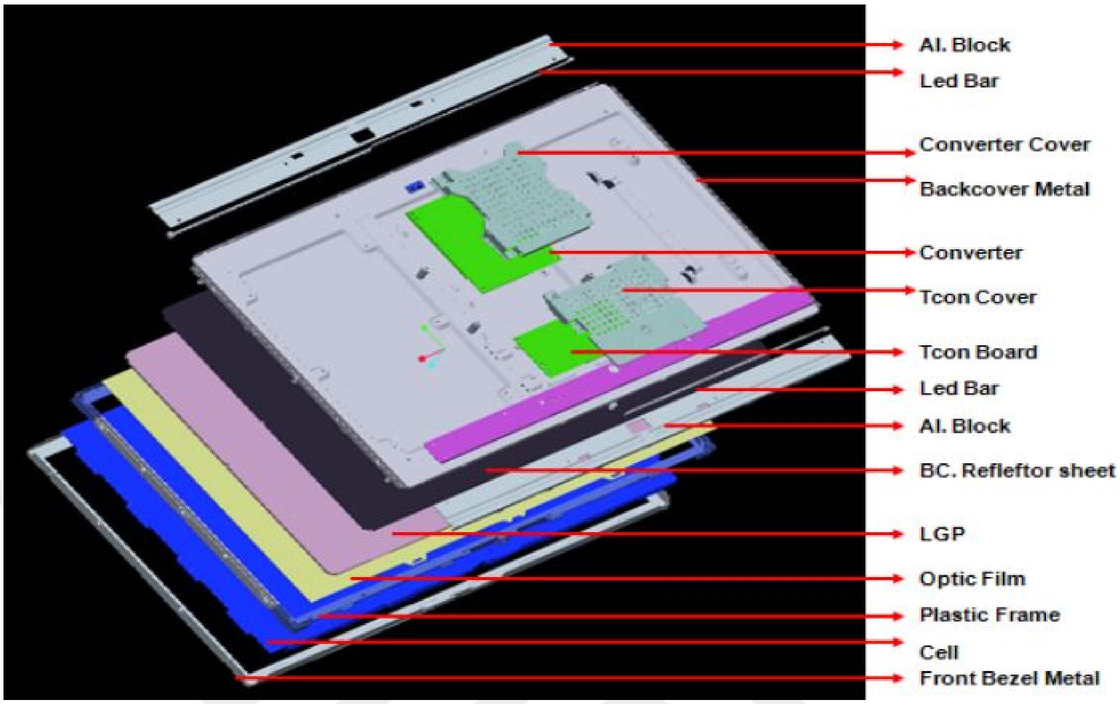

Figure 3: Inside structure of LCD TV[9]

Electric current is applied to these crystal pixels to obtain images[9]. The color and transparency of the pixels are changed by increasing or decreasing the electric current[9]. Back-light is used because pixels do not have their light source. When CCFL (cold cathode fluorescent lamp) is used as back-light, it is called CCFL LCD TV. If LED is used as a back-light, it is called LED LCD. Since CCFL LCD TVs provide illumination with fluorescent lamps, they have a thicker structure and high power consumption. Led LCD TVs can be designed in a slimmer structure and have low power consumption because the LEDs consume less power. LCD TVs feature high resolution but low contrast ratio[10]. Because the LCD panel is very thin, it is sensitive and easily broken[10].

It is a thin semiconductor material in nano sizes called Quantum dot(QD) in quantum dot-based light-emitting diode(QDled) TVs as shown in Fig.4.

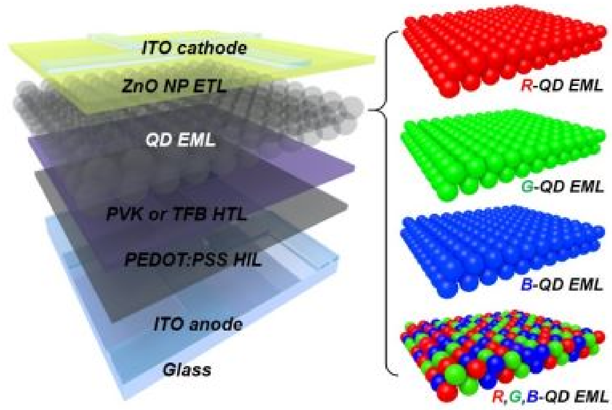

Figure 4: Optical film structure of QLED[11]

QD films that can be applied to the LED LCD TV to provide higher brightness. If QD film is applied directly, its luminous level decreases. Either the backlight brightness level should be increased to raise the luminous level or a special optical film should be used as shown in Fig. Colors are brighter and sharper according to normal LCD TVs[11].

It can be said that the mini-led technology is an upper segment of Led LCD TVs. The backlight structure uses smaller LEDs instead of large LEDs. Smaller LEDs can be divided into different zones and each zone can be controlled independently from each other. The image can be obtained a sharper and brighter appearance by using this structure type.

OLED (Organic Light-Emitting Diode) panels can emit their lights without using a backlight[12]. it may be possible to make thinner designs than Led TVs with the absence of a backlight structure as shown in Fig.5.

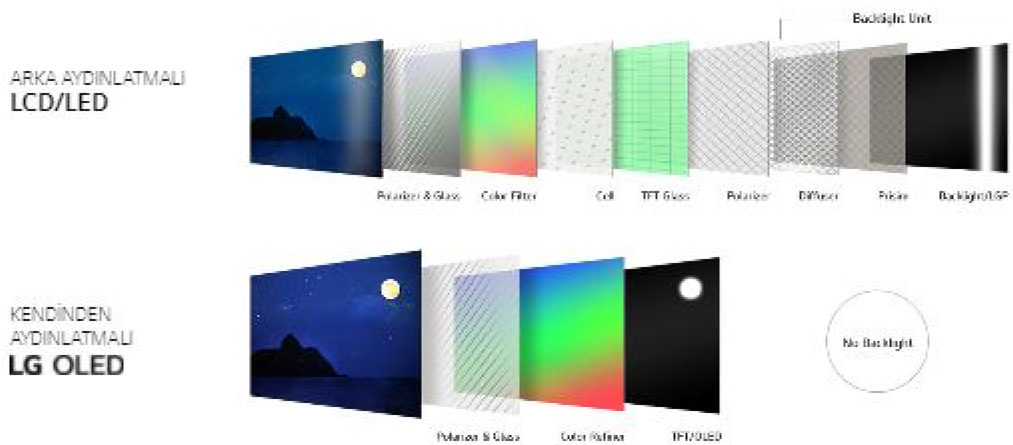

Figure 5: Structures of LED TV and OLED TV[12]

OLED TVs offer the opportunity to see black more black because they have a self-luminous structure[12]. This indicates that OLED TVs have higher contrast ratios. OLED TVs have lower power consumption and wide viewing angles[12]. Transitions between pictures are faster than LCD TVs. OLED panel prices are more expensive in the current market. In the future, with the development of technology, costs may decrease and remain in a more suitable price range.

OLED and similar products have increasing power requirements with more brightness and features. It can be answered with different topologies or methods to transfer higher power in small sizes. It is like the heart of a transformer for power supplies, which is the main element in power transfer. In this study, the voltage and current are generated for OLED panels. Interleaved power factor correction(PFC) and LLC resonant topologies are used on the power supply. It is aimed to keep the transformer performance in a more safe zone with higher power transfers and different transformer structures.

In order to respond to increasing power consumption, high efficiency was obtained and different transformers are used in this design. EFD, EE, etc. type transformer is generally used for LLC resonant topologies. Because the leakage of the transformer is used as a resonant coil. PQ, POT, etc. transformer is used to obtain distributed leakage inductance. In our investigations, the most heated point of the transformer is the leakage inductance regions. In high power transfers, the leakage ınductanec gets warmer and reaches risky levels as reliability. In the thesis study, power transfer is performed using the toroidal transformer by taking the leakage inductance out of the main transformer. The leakage ınductance of toroidal transformer is designed as minimum as to prevent the overheating for toroidal transformer. The resonant coil is provided with another small coil.

CHAPTER II

LITERATURE REVIEW

2.1 Switching Methods

Hard switching, snubber circuits, and soft-switching methods are used to control the switching elements. The switching losses can be greatly reduced with these methods which vary according to the topology. The switching losses on the MOSFET can be greatly reduced with the soft-switching method as shown in Fig.6[13].

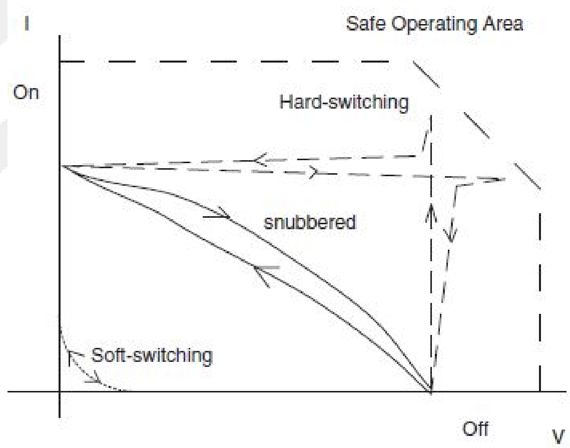

Figure 6: Typical Switching Transitions[13]

Hard switching, snubber circuits, and soft-switching methods are used to control the switching elements. Switching losses can be greatly reduced with these methods which vary according to the topology. Switching losses are decreased with the soft-switching method as shown in Fig.6. There are some effects that the designer cannot prevent due to the internal structure of the MOSFET. These effects occur in the production of MOSFET. The capacitance effect is observed in the internal structure of the MOSFET as shown in Fig.7. These capacitance effects affect the losses on the switching element.

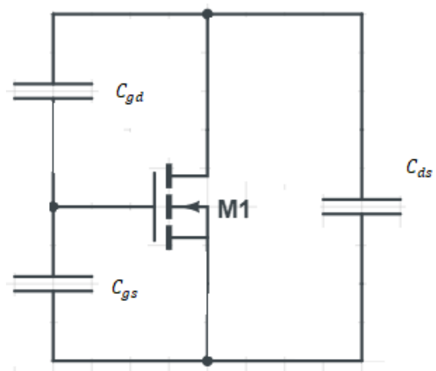

Figure 7: Internal Structure of MOSFET

$$InputCapacitor \quad C_{iss} = C_{gd} + C_{gs} \tag{1}$$

$$MillerCapacitor \quad C_{rss} = Cgd \tag{2}$$

$$OutputCapacitor \quad Coss = Cds \tag{3}$$

Internal capacitance values are calculated at Eq.(1), Eq.(2), Eq.(3).If the input capacitor is selected as small as possible, it provides an advantage for the switching loss. When the gate signal is applied to the MOSFET, the waveform of the switching element is shown in Fig.8.

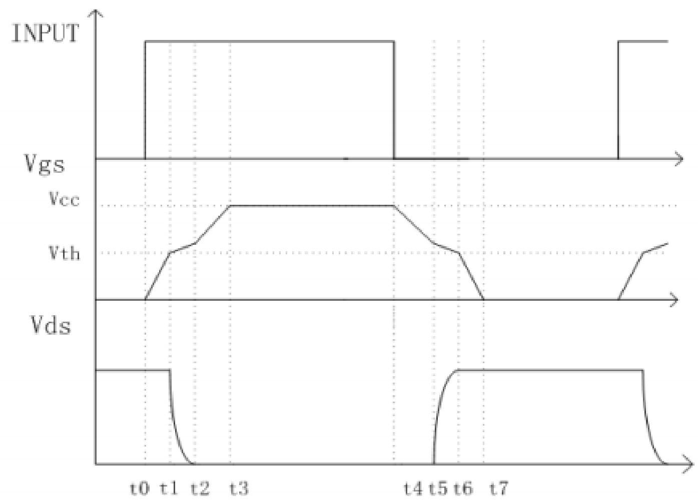

Figure 8: Curve of MOSFET Signals[14]

C_{gs} capacity starts to charge in time interval t0-t1. In the time interval t1-t2, the MOSFET V_{th} has reached and opened. C_{gd} capacitor causes this time interval which is called the miller effect[14]. Length of time in all these transition moments causes losses on the MOSFET. These values should be selected to reduce losses in designs.

2.1.1 Hard Switching

In the hard switching technique, there are situations where the current and voltage stay at a certain level during the opening and closing. For this reason, large losses occur in opening and closing, which causes the material to heat up and large noise effects. Hard switching is used for some topologies because it is designed without the use of extra materials and brings low cost, as well as providing space in the design and easy controllability. The turn-on and turn-off waveforms for hard switching are shown in Fig.9[15].

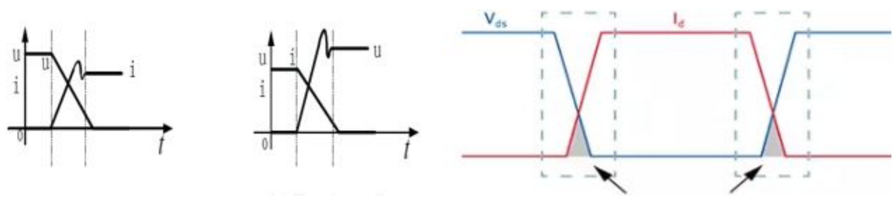

Figure 9: Turn-on and turn-off waveforms for Hard switching[15]

High di/dt and dv/dt values which occur due to suddenly the change of voltage and current create high electromagnetic interference(EMI). EMI noise must be eliminated at its source. High di/dt may cause overvoltage in power converters due to leakage inductance. High dv/dt can create leakage current in magnetic elements due to leakage capacitive coupling between windings. There are several methods reduce EMI noise such as snubber circuit, reducing the inductance values of the circuit paths, adjusting the switch open and close times or using the soft switching method.

2.1.2 Soft Switching

In the hard switching method, as the frequency increases, the switching losses also increase. This allows to go up to a certain frequency in design. It is advantageous to reduce the passive components by increasing the frequency. Soft switching methods are used to reach high powers and reduce switching losses. Soft switching can be done with ZVS (Zero Voltage Switching) or ZCS (Zero Current Switching) methods. Usually, the ZVS method is preferred for designs with high voltage and the ZCS method is generally preferred for designs with high current. Fig.10 represents zero crossings of ZVS and ZCS signal.

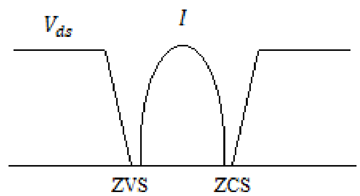

Figure 10: ZVS and ZCS Waveform

Switching is done at zero crossings of the ZVS voltage. ZCS is switched at zero crossings of the current. Switching loss is eliminated at the zero value transition of voltage or current. Soft switching methods provide a great advantage in EMC tests. There are many factors in design that affect EMC tests.

2.2 Conventional Isolated DC-DC Converters

2.2.1 Fundamental Isolated DC-DC Converters

Direct Current(DC)-Direct Current(DC) converters can be evaluated in two groups; the first is isolated power supply, the second is non-isolated power supply. In consumer electronics such as TVs, an isolated power supply is generally used to prevent electric shock to the end-user. One of the most important criteria in designing is the determination of the topology. It is necessary to determine the topology according to the power requirement of the system. The table below gives approximately power levels according to topologies.

The power levels for topologies are shown in Tab.1[16]. These results are determined approximately, so higher or lower power levels can be achieved by using different components.

Table 1: The fundamental topologies according to power levels

Topology	Power(W)	Typical Eff.	Max. Duty	90-270VAC Inp.
DCM Flyback	150	75	0.9	Yes
Forward	150	75	0.45	Yes
Push-Pull	500	80	0.45	No
Half-Bridge	500	85	0.45	Yes
Resonant LLC C.	500	90	0.45	Yes

Flyback topology is a commonly used topology in isolated topologies. It uses a single switching element without using an extra inductor on the secondary side. This is a pretty low-cost topology. However, several disadvantages are the temperature problems on the transformer and extra capacity usage due to high ripple currents. The power is transferred in a single cycle. The forward converter is very similar to the flyback topology but does not store energy while the switch is in transmission[17]. It transfers the energy directly to the output.

Topologies such as Push-pull, Half-bridge, LLC resonant converter transfer the power by using double switching. In this way, the transformer core is used completely to transfer the power in the negative and positive cycles. In a push-pull converter, the switching element periodically reverses the current on the transformer. The power is stored on the output inductor and capacitor to use by the load. For the push-pull topology, an extra winding is required since power is transferred with two windings on the primary side. A Half-bridge converter can be examined under two headings; Asymmetric half-bridge converter, symmetric half-bridge converter. The asymmetric half-bridge converter is preferred more to use in applications which have low voltage and high current requirement. The half-bridge LLC topology has generally above 90 percent efficiency. Even if a synchronous rectifier is used instead of output diodes, this level can reach 95 percent. It has wide application areas such as consumer electronics, battery chargers, led lighting, etc.

2.2.2 Basic Resonant Converters

Resonance is the oscillation of a system in higher amplitude at a certain frequency. The resonant frequency is called the point where the values of capacitance and inductance in an LC circuit are the same and in opposite directions. So the total reactance is equal to zero. At this point, the electrical current is maximum. In this circuit structure, the magnetic energy of the coil transforms into the electrical energy of the capacitor. The coil and capacitance values determine the cycle period. The reactance of capacitance and inductance are calculated as;

$$Xc = 1/jwC, Xl = jwL \tag{4}$$

Impedance versus frequency graph is represented for LC circuit in Fig.11.

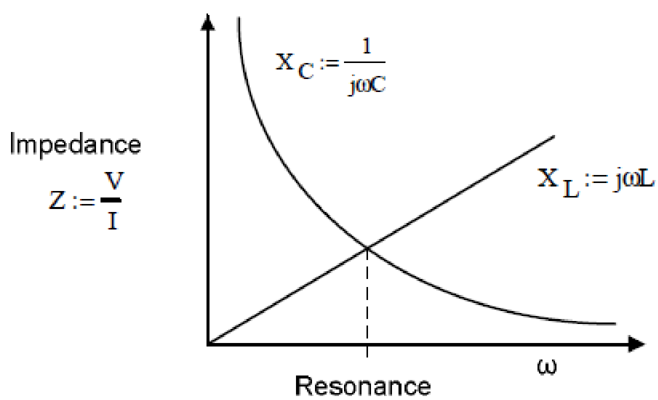

Figure 11: Resonat Frequency for LC circuit

The current waveform is created close to sinusoidal in resonant converters, unlike traditional switch mode power supply(SMPS) topologies. This waveform is transferred to the secondary side with the transformer and fed the load. Fig.12 represent general block diagram for resonant converters.

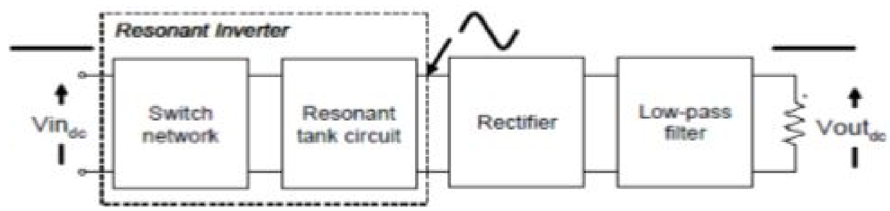

Figure 12: General Block diagram for resonant topologies

Fig.12 represent general block diagram for resonant converters. Resonant converters switch current and voltage at zero or near zero, so switching losses are low. It can run at high frequency due to low switching losses. It enables a smaller-sized card design that has more power in the design. Resonance converters have high efficiency due to their low losses. They are preferred due to their good EMI performance in industrial applications.

2.2.2.1 Series Resonant Converter(SRC)

In the serial resonant converter, L (inductor) and C (capacitor) are connected in series on the primary side of the main transformer as shown in Fig.13.

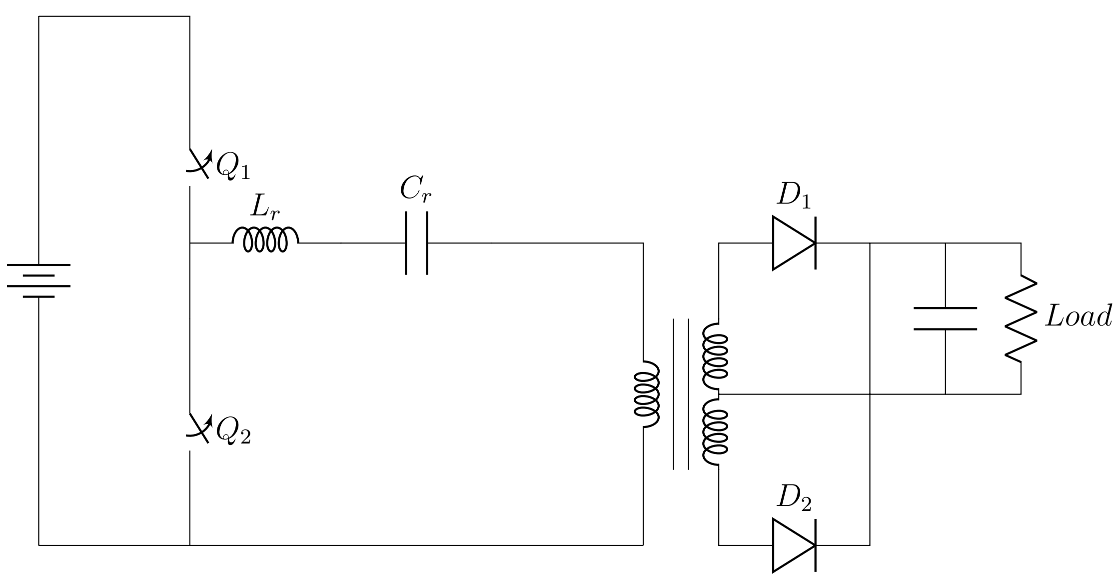

Figure 13: Series Resonant Converter

Resonant tank circuit and load are series to each other. In a series circuit, a voltage appears as a divider and DC gain is always below 1[18]. When the input voltage increases, the system starts operating further away from the resonant frequency. As the frequency increases, the total impedance of the tank increases and the energy circulating in the tank increases[18]. As a result, the MOSFET turn-off current also increases and a heating problem occurs on MOSFET. The gain versus frequency graph for the series resonant converter is shown in Fig.14[19].

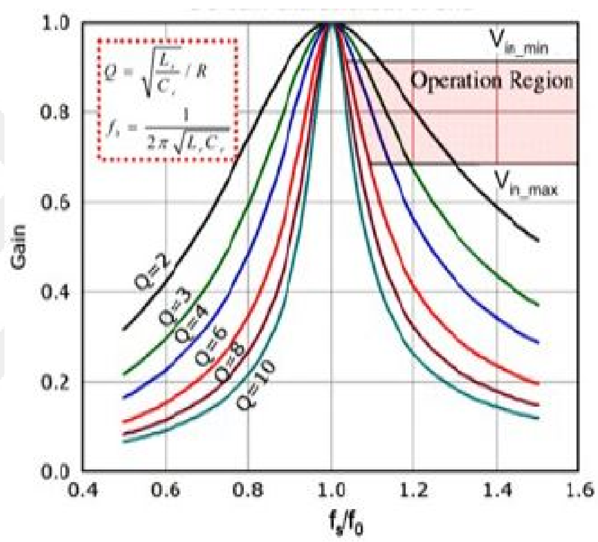

Figure 14: Gain versus frequency graph for series resonant converter[19]

On the left side of the resonant frequency, under resonant system Zero Current Switching (ZCS), on the right side of the resonant frequency, the system operates as Zero Voltage Switching (ZVS)[20]. For a MOSFET, ZVS is preferred and EMI emission is less. At the resonant frequency, the resonant tank impedance is minimum and DC gain is maximum. It operates under no load, but the output voltage is irregular. It needs to increase the switching frequency to regulate the output voltage. Its performance is good at one operating point. It is not efficient in the wide input range and output voltage variation[20].

2.2.2.2 Paralel Resonant Converter(PRC)

In a parallel resonant converter, L and C components are used on the primary side and C is parallel to the load as demonstrated in Fig.15. Therefore, it is called a parallel resonant converter.

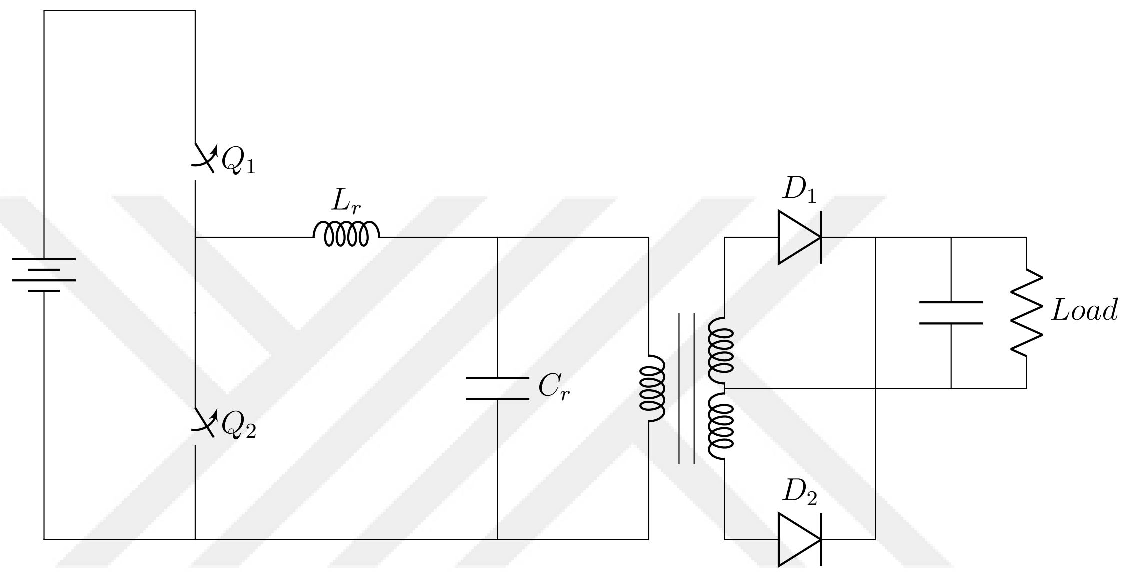

Figure 15: Paralel Resonant Converter

The resonant circuit is connected in parallel with the load and acts as a kind of voltage source. Output coil is put on secondary side to match the impedance. The increase in input voltage increases the circulating energy like the series resonance converter. The gain versus frequency graph for the parallel resonant converter is shown in Fig.16.

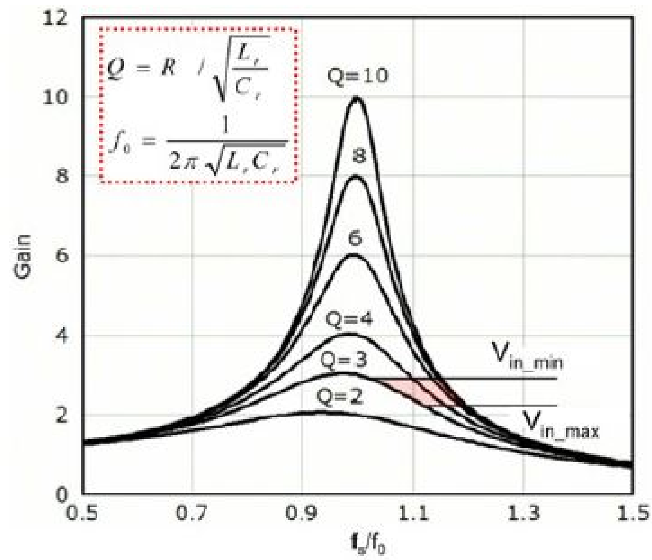

Figure 16: Gain versus frequency graph for parallel resonant[19]

Maximum gain is at the resonant frequency which has minimum impedance. Unlike the serial resonant, the gain is greater than one in this application. The right side of the resonant frequency is ZVS in the over resonant, and ZCS is applied on the left side of the resonant frequency. When the working frequency is further away from the resonant frequency, more circulating energy circulates than the serial resonant[20]. The increase in turn-off currents increases switching losses and so the parallel resonant is less efficient topology than series resonant[20]. It has a small operating bandgap and narrow frequency-changing according to series resonant frequency[20].

2.2.2.3 LCC Resonant Converter

LCC series-parallel resonant converter is designed by using one inductance and two capacitors on the primary side as demonstrated in Fig.17. L and C are connected in parallel to each other. Another capacitor is in series to LC and the load.

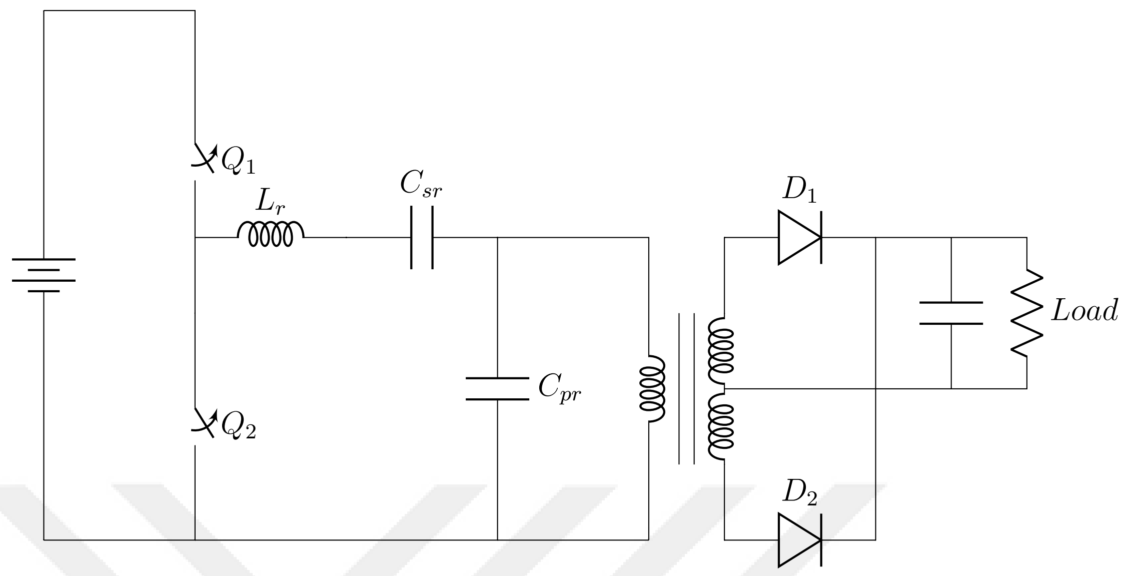

Figure 17: LCC resonant converter

LCC resonant converter is a combination of the serial resonant converter and parallel resonant converter. Output coil is put on secondary side to match the impedance. When the input voltage increases, circulating energy increases, but this energy is higher than SRC and lower than PRC. The gain versus frequency graph for LCC resonant converter is shown in Fig.18.

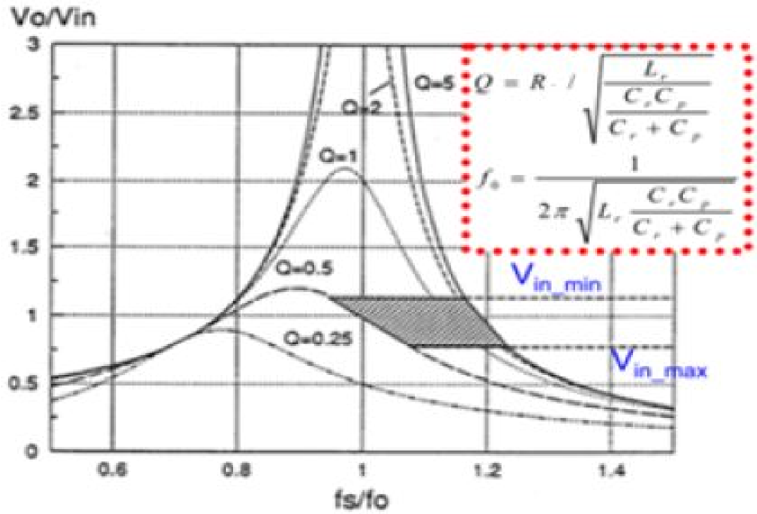

Figure 18: Gain versus frequency graph for LCC resonant converter[19]

There are two resonant frequencies in the LCC converter. The first resonant frequency is between Lr and Csr, the second resonant frequency is between Lr and Cpr. When the quality factor (Q) increases, the voltage gain peak shifts towards the other resonant frequency. The right side of the second resonant frequency allows doing ZVS.

2.3 LLC Resonant Converter

The LLC resonant converter has two inductance Lm, Lr, and one capacitance Cr on the primary side as shown in Fig.19. Although the LLC resonant converter is very similar to the serial resonant converter, it can be called the advance of the serial resonant converter.

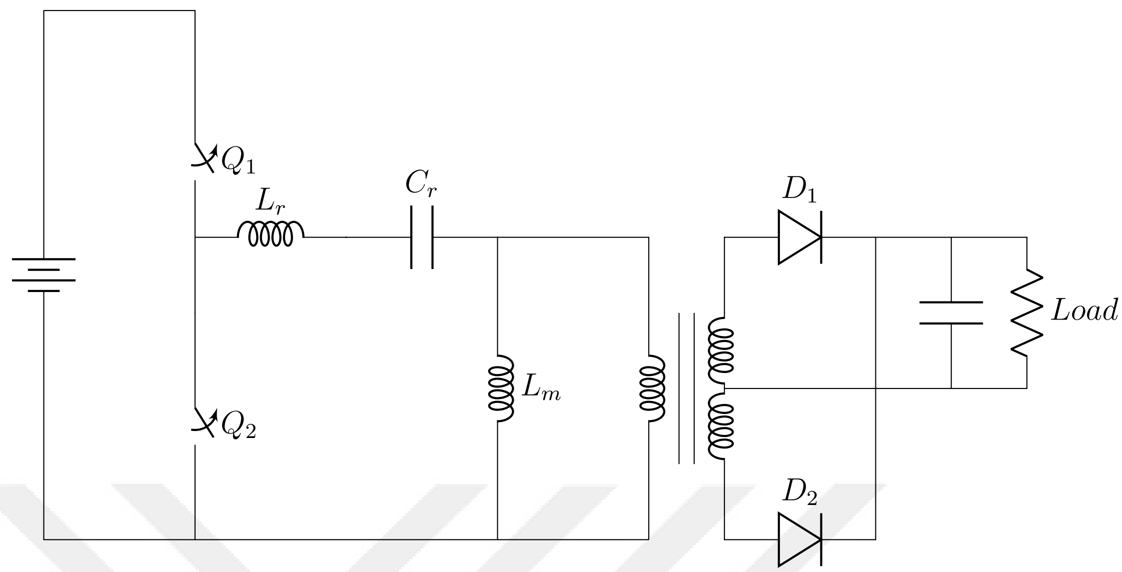

Figure 19: LLC resonant conveter

In series resonant, parallel resonant and LCC resonant converters, high circulation energy and high switching loss occur at high input voltage [21]. The best efficiency is obtained at the resonant frequency. Working on over resonant or under resonant frequency may cause some losses on the converter. The LCC and LLC converter has two resonant frequencies. it is more efficient to work at the highest resonant frequency [21]. For high efficiency, the system is operated at the closest resonant frequency. The gain versus frequency graph for LLC resonant converter is shown in Fig.20.

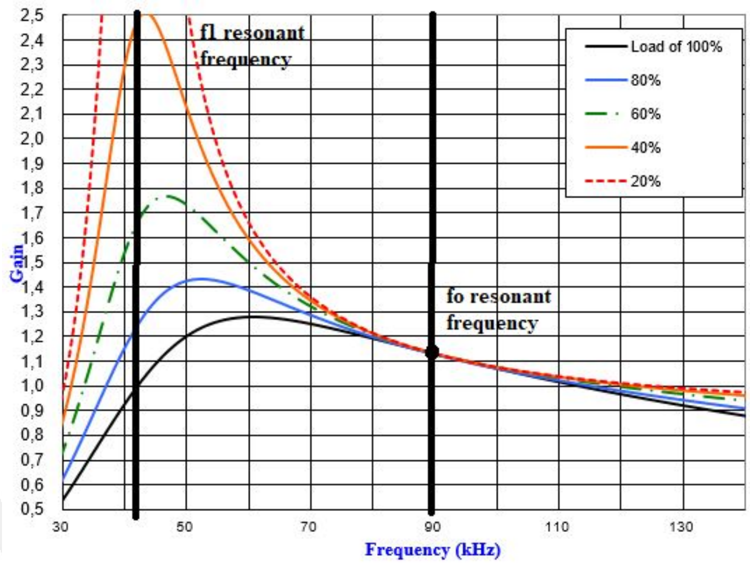

Figure 20: Frequency versus gain graph for LLC resonant converter

By using LLC resonant converter topology, high efficiencies of 95 and 96 percent have been achieved with different designs[22][23]. It is aimed to minimize secondary losses by using a synchronous rectifier. The LLC converter efficiency was aimed at 96 percent by reducing the switching losses.

CHAPTER III

DESIGN OF CONSIDERATION

3.1 Elecromagnetic Interference(EMI) Filter and Inrush Current Limiter

In this part of the thesis, each section of hardware design will be examined. The general blog diagram is shown in Fig. 21. The PCB design is shown in the appendix stage for general circuit design. The hardware study is designed to operate between 100VAC-270VAC input voltage range and 50-60Hz frequency range. If the general block diagram is approximately explained, the AC signal passes through the rectifier block and a full-wave rectified signal is obtained. This signal is boosted to the level of 390VDC and also power factor correction is performed in the PFC stage. In the LLC stage, 390VDC signal is transferred to the secondary side with transformer and a 24VDC signal is obtained after passing through the synchronous rectifier.

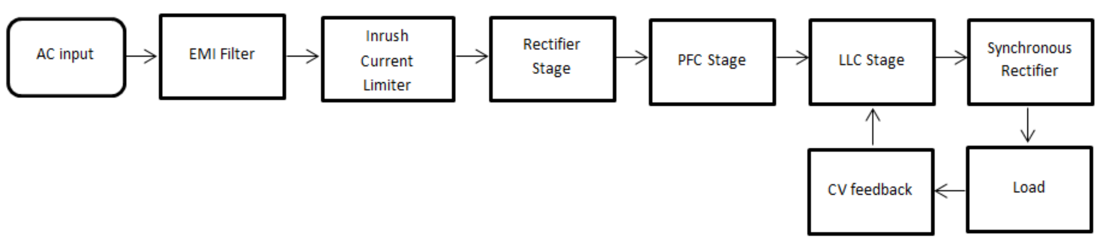

Figure 21: General block diagram of hardware design

EMI filter block is used to suppress the emitted noise by the switching elements. Since the switching elements operate at 100kHz in the design, a suitable filter element should be selected to suppress that frequency band and its harmonics. Two noise sources are happening after the switching. These are conducted noise and radiated noise. Conducted noise is the transmitted noise via cable, printed circuit board(PCB) traces, parasitic capacitance, etc., and measured from the input network. Radiated noise is the emitted noise by the card and measured with the antenna. The general circuit diagram for the EMI stage and PFC stage is depicted in Fig. 22.

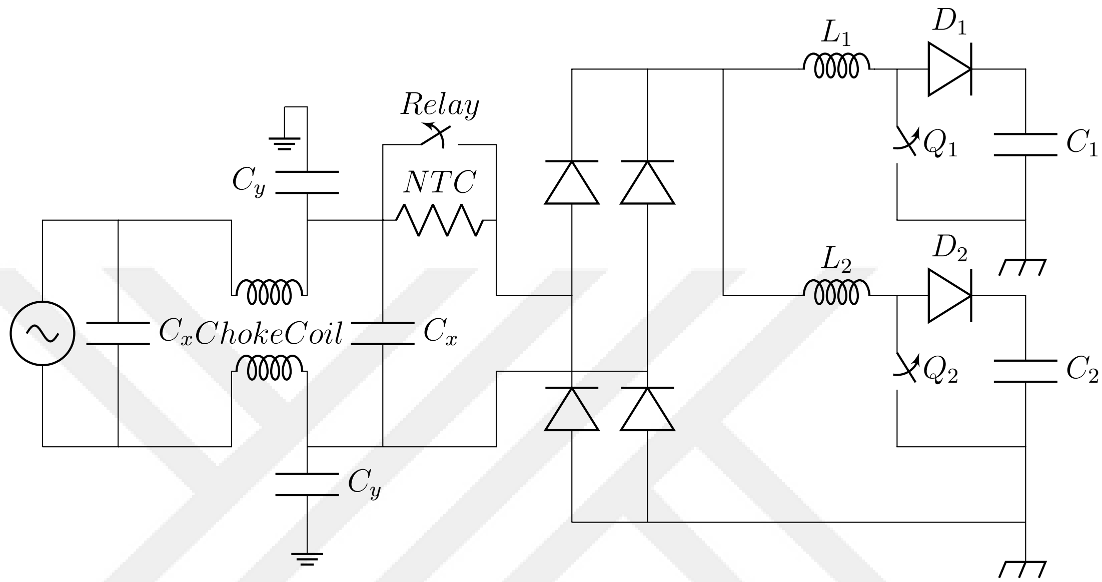

Figure 22: General circuit diagram for input stage

There are two types of noise among the switching elements: differential mode and common mode. For the Differential mode, the noise is on the phase-neutral line flows in different directions. For common mode, the noise is on the phase-neutral line flows in the same direction. EMI filter block is designed as a C-L-C-L-C structure to suppress the noise.

At the first turn-on, high-value bulk capacity draws a high current from the grid during the charging. The high current is called inrush current. If nothing is placed to prevent high current, it may damage the semiconductor materials. The instantaneous charging current of the capacitor is shown in Eq.(5).

$$I_c = C\frac{dV_c}{dt} \tag{5}$$

NTC (Negative Temperature Coefficient) or resistor is used to prevent this current.

NTC was preferred in the design. Since the design has 384W output power, high currents pass through the NTC at 100VAC signal. High currents may damage the NTC due to over-temperature. The NTC is bypassed by a relay after a certain time. Thus, A high loss on NTC is prevented with by-passed.

3.2 Power Factor Correction(PFC) Stage

The power factor is mathematically expressed as the angle between real power and apparent power as shown in Fig. 23. Real power is consumed due to resistive load and does the actual work such as lighting, the image on TV, etc. Reactive power is consumed for the formation of the magnetic or electrical field to make real power.

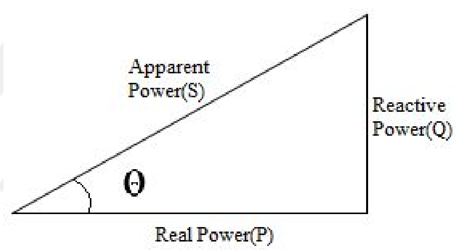

Figure 23: Relationship of powers to PF

Total power is called the sum of reactive power and real power. Power factor is the ratio between real power and apparent power. The power factor correction stage is used to use energy efficiently in the design. The power factor (PF) value is designed to be between 0.95-0.99 in the study. First of all, the AC signal is rectified. The rectified signal is the input signal of the PFC stage. The signal is boosted up to 390VDC with different switching frequencies. The DC signal is obtained with bulk capacitors. Bulk capacitors are also enabled SMPS to operate at hold-up time. If the capacitor is chosen too large, the peak current values that are required for charging will increase since the charging time is decreased. A maximum ripple voltage is allowed between 5%-10% in the design.

$$\Delta V_{out(p-p)} = \frac{P_{out}}{2\pi.f_{line}.C_{bulk}.V_{out,nom}} \tag{6}$$

$$I_{c(rms)} = \sqrt{\frac{P_{out}^2.16.\sqrt{2}}{9\pi.V_{in(rms)}.\eta.V_{out,nom}} - \frac{P_{out}^2}{V_{out(nom)}^2}} \tag{7}$$

$$t_{hold-up} = \frac{C_{bulk}.(V_{out}^2. - V_{out(min)}^2)}{2.P_{out}} \tag{8}$$

In the design, the maximum ripple voltage is set at 10 percent. By using Eq.(6), the bulk capacitor value was determined as 300uF. The maximum ripple current can be calculated by using Eq.(7). The ripple current can be reduced for a capacitor by adding other capacitors. The hold-up time was calculated ass 56ms by using Eq.(8).

it is necessary to approach the input current shape to the sinus to bring the power factor(PF) to one. The boost converter topology is used for the power factor correction. Interleaved boost converter structure is preferred due to the high power and slim design.

The input operating voltage of the power card is between single-phase 100VAC-270VAC. The input voltage of the PFC section is in the rectified signal of 100VAC-270VAC and the output voltage should boost to a constant 390VDC level. When the input voltage is low as 100VAC input, the temperature stress is high for the PFC stage due to high current stress. Interleaved PFC application was chosen for high power requirement, slim design and to control the temperature.

NCP1631 two-phase interleaved power factor controller is used in the design. Interleaving consists of two small PFC stages according to a bigger design. The Interleaved PFC stage provides the use of smaller components and distribution of heating. The package of the PFC controller is SOIC-16. It drives two blocks with a 180 phase difference[24]. The functional block diagram of the PFC controller is shown in appendix Fig. 77.

A boost converter consists of a switching element, coil, diode and capacitor. When the switch is on, energy is stored in the coil and the coil current increases. When the switch is off, the stored energy on the coil is transferred to the load and the coil current decreases. If the coil current is continuously positive, it is called conduction mode. If the coil current drops to zero, it is called discontinuous mode. If it comes to zero cuts and immediately switches on, it is called critical conduction mode. The boost stage is run for a light load in discontinuous mode. When the load is heavy, the boost stage is run in critical conduction mode[25]. The coil current of the boost converter is shown in Fig. 24.

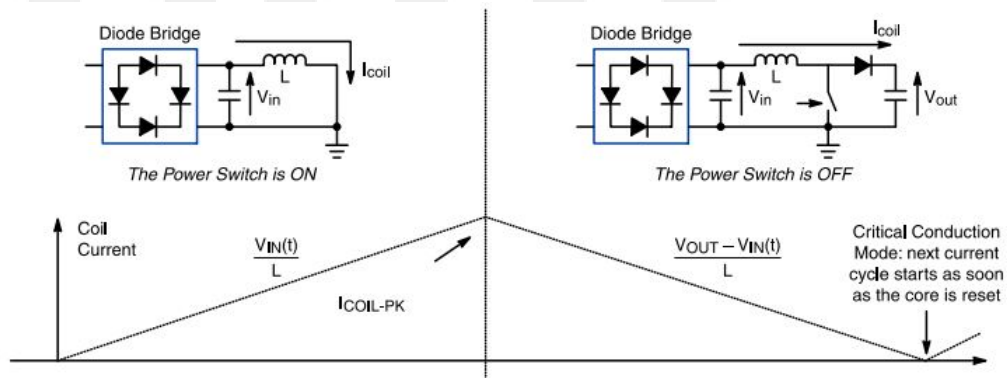

Figure 24: States of operation for critical conduction mode[25]

By using Eq.(9) and Eq.(10), the coil current was calculated as the root mean square(RMS) 2.49A, peak 6.1A. The minimum inductance was calculated as 123 uH by using Eq.(11). 180uH coil was used in the design.

$$I_{L(peak,max)} = \frac{\frac{2.\sqrt{2}P_{in(max)}}{2}}{V_{in(rms)_{min}}} \tag{9}$$

$$I_{L(rms,max)} = \frac{I_{L(peak,max)}}{\sqrt{6}} \tag{10}$$

$$L > \frac{V^2_{in(rms,min)}.(V_{out} - \sqrt{2}.V_{in(rms,LL)})}{P_{in(avg)max}.V_{out,nom}.f_{sw(max)}} \tag{11}$$

Unlike the standard boost converter, a boost converter operating at different frequencies is used to perform power factor correction. The frequency increases at the breaking point of the switching element because fewer current peaks are required. The frequency is decreased when high coil currents are needed at the peak point. Thus, a sine wave following the input current is obtained. The PF factor is between 0.95-0.99. Fig.25 shows the ınductor waveform during the switching.

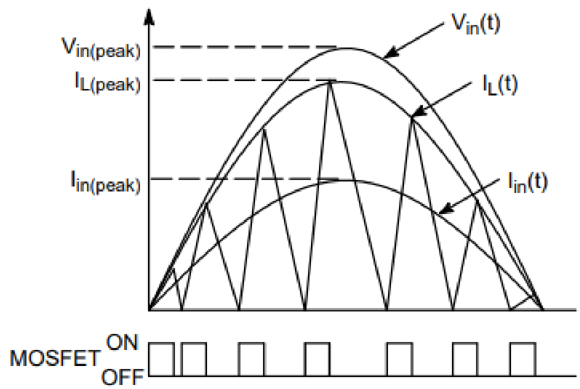

Figure 25: Inductor Waveform During Critical Mode Operation[26]

The Vcc requirement for the integrated circuit(IC) is provided by auxiliary winding. Zero current detection(ZCD) pin detects zero current detection[26]. It follows the zero crossings of the coil current with the help of the extra coil which wraps on the PFC coil. For the Zero current detection winding, the rate of winding is calculated in Eq.(12).

$$N < \frac{V_{out} - (\sqrt{2}V_{in(rms,max)})}{0.5} \tag{12}$$

Feedback is taken from the output via a voltage divider resistor and the output is kept at a fixed voltage at 390V. Maximum on time is determined with the RT pin. The circuit schema diagram for the PFC stage is shown in Fig. 26.

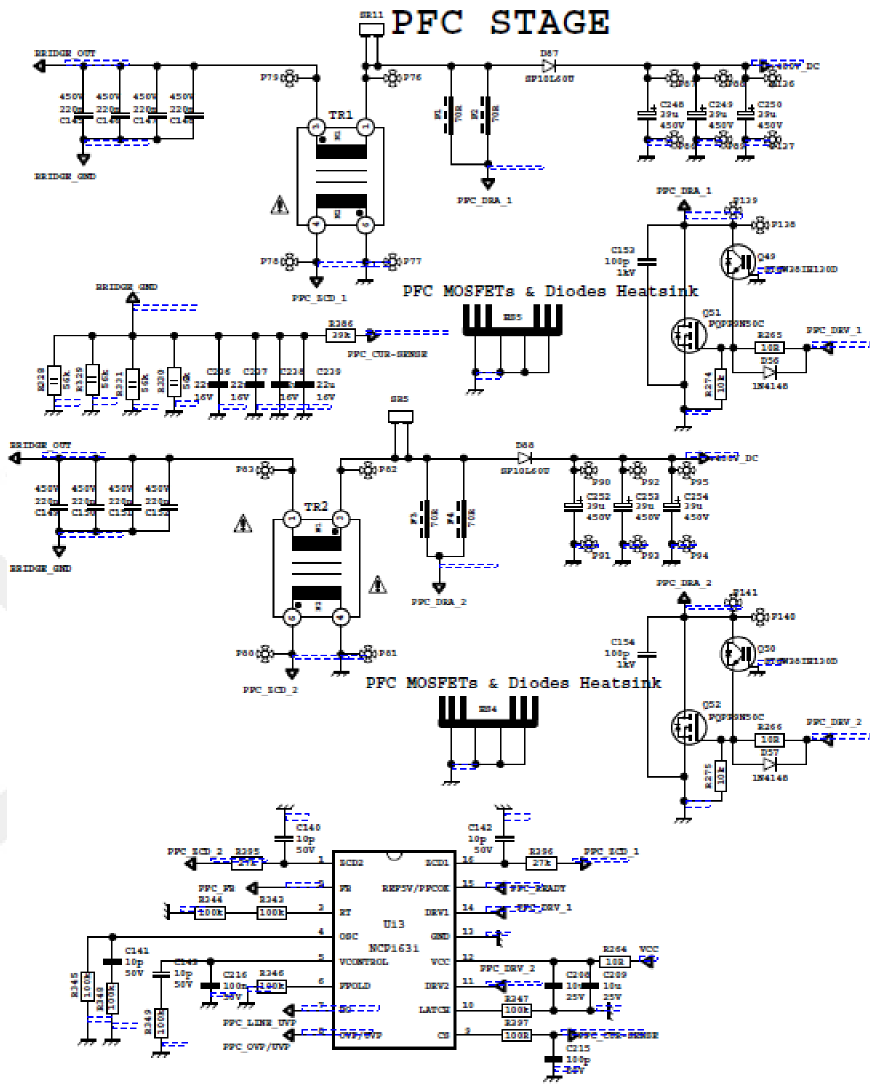

Figure 26: Circuit schema for PFC stage

3.3 Synchronous Rectifier Stage

A synchronous rectifier is used instead of schottky diodes by driving synchronous MOSFETs on the secondary side [27]. Diodes have high Vf values. When the high current passes through them, heat problems and low efficiency occur on the power supply unit. The synchronous rectifier is used for high-efficiency card design with low Rds-on MOSFET[27]. The efficiency is aimed at 96 percent for the LLC resonant stage.

Two synchronous ICs are used to drive MOSFETs for a negative and positive cycle at the center-tapped rectifier. The name of the synchronous IC is ZXGD3104N8. Synchronous IC includes differential amplifier detector stage and high current driver stage[28]. A functional block diagram of synchronous IC is shown in Fig.27.

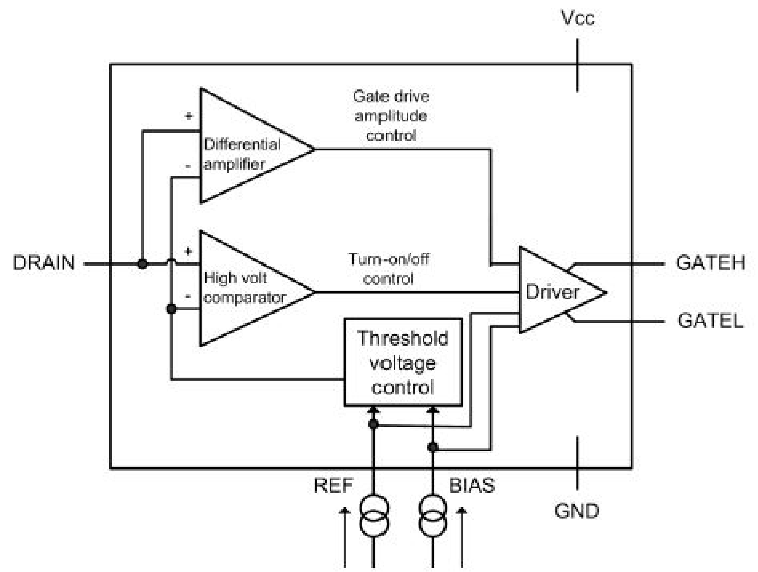

Figure 27: Functional block diagram of synchronous rectifier[28]

Synchronous IC supports up to 250kHz [27]. Firstly, the controller monitors the drain-source voltage of the MOSFET. As soon as the transformer starts to transfer the energy, the current flows through firstly the body diode of the MOSFET. When the body diode is activated, the drain-to-source voltage of MOSFET occurs approximately 0.8V. This voltage value is equal to the forward voltage of the body diode. The controller detects the voltage to open the MOSFET proportionally. When the drain current of MOSFET is decreasing to zero, the zero current switchings (ZCS) method is activated to drive the MOSFET at zero crossings. The switching losses on the MOSFET are also reduced with the zero current switching(ZCS) method. The detailed timing diagram is shown in Fig.28.

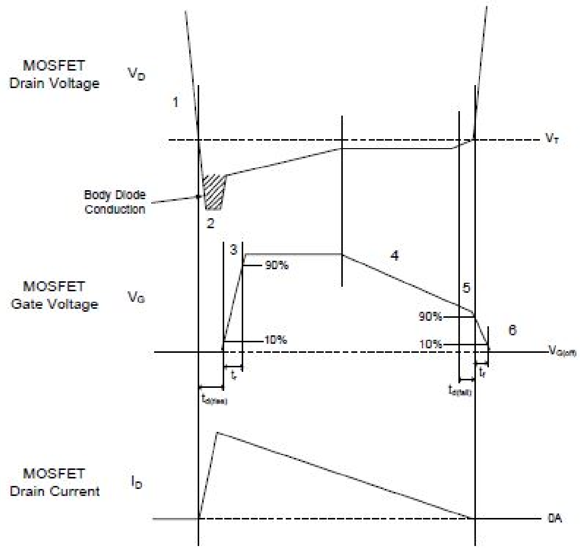

Figure 28: Timing diagram of synchronous controller[28]

The currents are divided by totally four MOSFETs. The temperature is distributed by using two MOSFETs in parallel for a cycle. Two parallel DPAK type MOSFETs are used. The circuit schema is shown in Fig. 29.

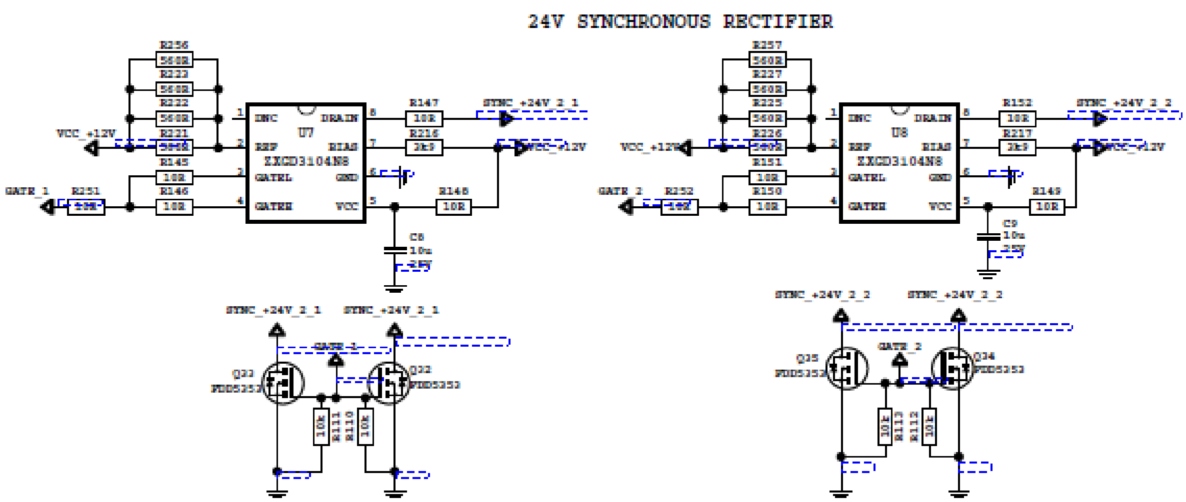

Figure 29: Circuit schema of synchronous rectifier

3.4 Detailed LLC Resonant Converter

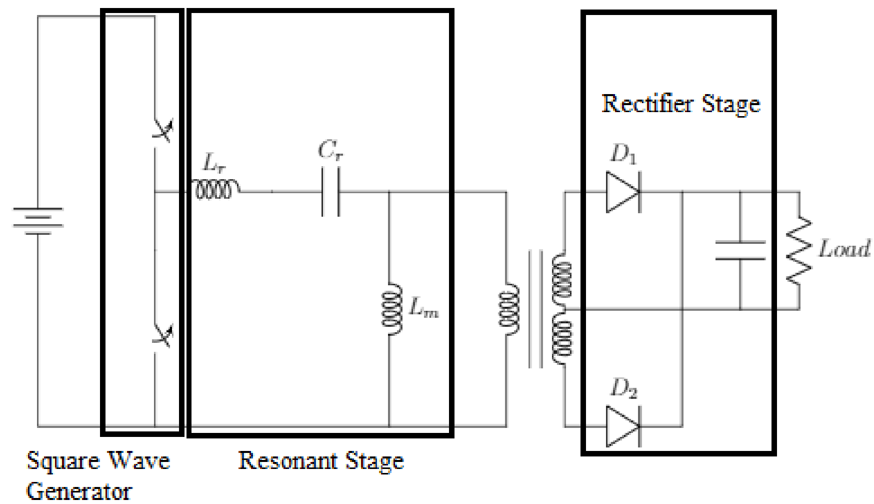

Figure 30: Three stages of LLC resonant conveter

LLC resonant converter consists of three main blocks which are a square wave generator, a resonant network, and a rectifier block. The square wave generator is happened by using Q1 and Q2 switching elements s shown in Fig. 30. They operate theoretically at a 50 percent duty cycle ratio. Vd voltage is generated as a square wave at the drain point of Q2 MOSFET. The resonant stage is consists of Cr (resonant capacitor), Lr (resonant inductance), and Lm (Magnatezing inductance of transformer) elements. It filters current harmonics and converts the current signal to a sinusoidal signal. The rectifier stage is consists of diodes or optionally MOSFETs. At the exit of the transformer, A DC signal is obtained by MOSFETs and capacitors. Lm is used as a transformer magnetizing inductance in the application. The resonant Lr coil can be used separately in different magnetic fields or integratedly in the same transformer. When a transformer is used in the design, the leakage inductance of the transformer is used as the resonant ınductance. In this study, the integrated transformer and separated transformer are designed and compared to each other.

3.4.1 Working Principle of LLC Resonant Converter

A general block diagram and waveforms for LLC resonant converter are shown in the following six figures[29].

In Phase 1, Q1 is in turn-off and Q2 is in turn-on. The stored energy on Cr and Ls provides the energy to the load. The current flows to the load through diode D2. This phase ends when Q2 is in turn-off.

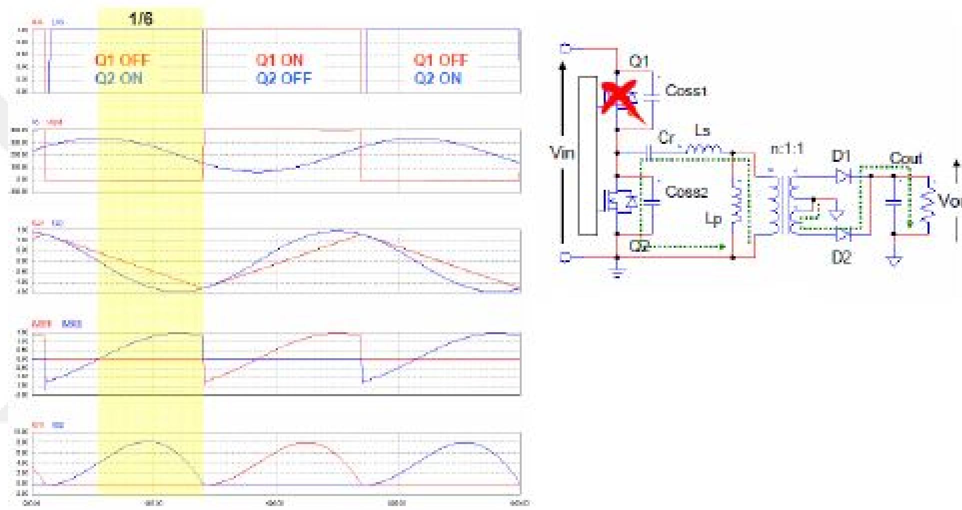

Figure 31: LLC Converter Working Principle for phase 1[29]

The phase 2 interval is called a dead time. Meanwhile, the two switching elements are in turn-off. In phase 2, Q1's body diode is in turn-on. The circulating current in the primary side charges Coss2 and discharges Coss1 until Coss1 is equal to Vin. When the Q1 MOSFET opens, ZVS occurs. In this phase, the load is fed the energy on the capacitor.

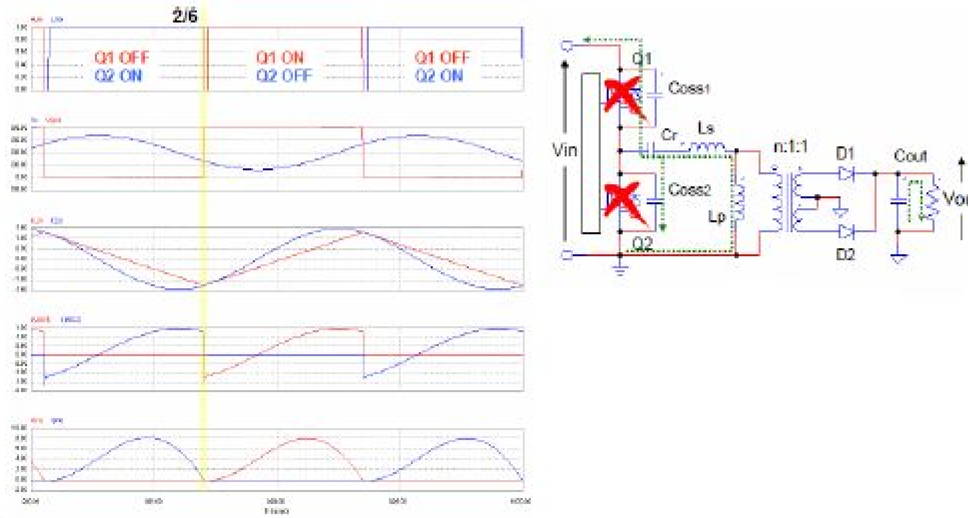

Figure 32: LLC Converter Working Principle for phase 2[29]

In this phase 3, Q1 is in turn-on and Q2 is in turn-off. The resonant current I goes through Q1's Rds-on via the resonant network. When the resonant current reaches zero, the phase is ended.

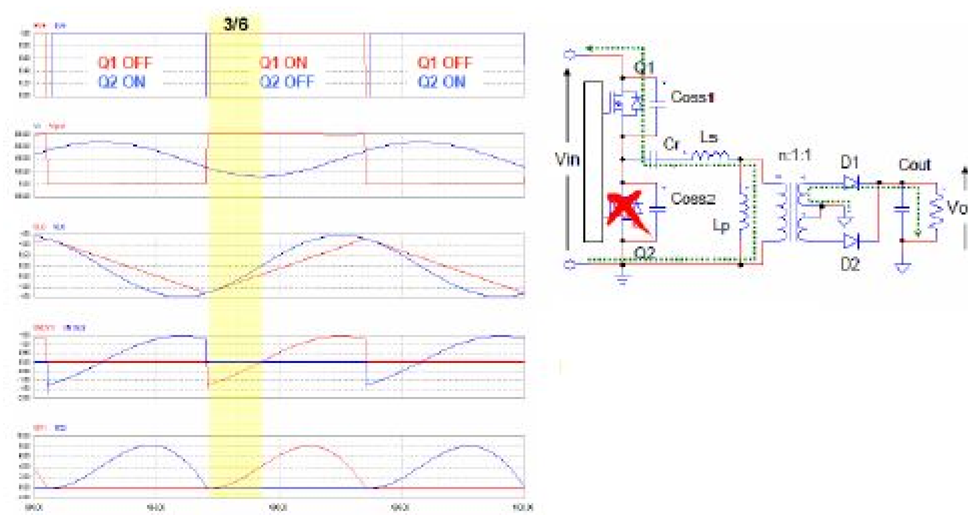

Figure 33: LLC Converter Working Principle for phase 3[29]

Ir current goes through Q1 Rdson to the resonant tank. When the Q1 is switched off, the loop is completed. Q2 is in turn-off during this period. The energy is transferred to the load through the D1 diode. Cr and Ls store and transferred the energy in this phase.

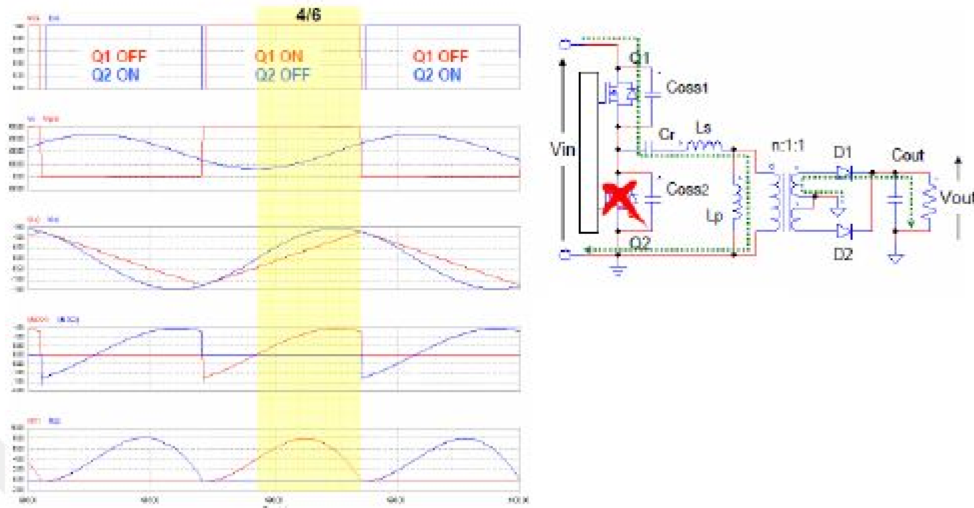

Figure 34: LLC Converter Working Principle for phase 4[29]

Phase 5 is a dead time to switch safely for another switching element. In phase 5, Q2's body diode is in turn-on. The circulating current in the primary side charges Coss1 and discharges Coss2 until the voltage of Coss2 is equal to zero. When the Q2 MOSFET opens, zero voltage switching(ZVS) occurs. In this phase, the load is fed the energy on the capacitor.

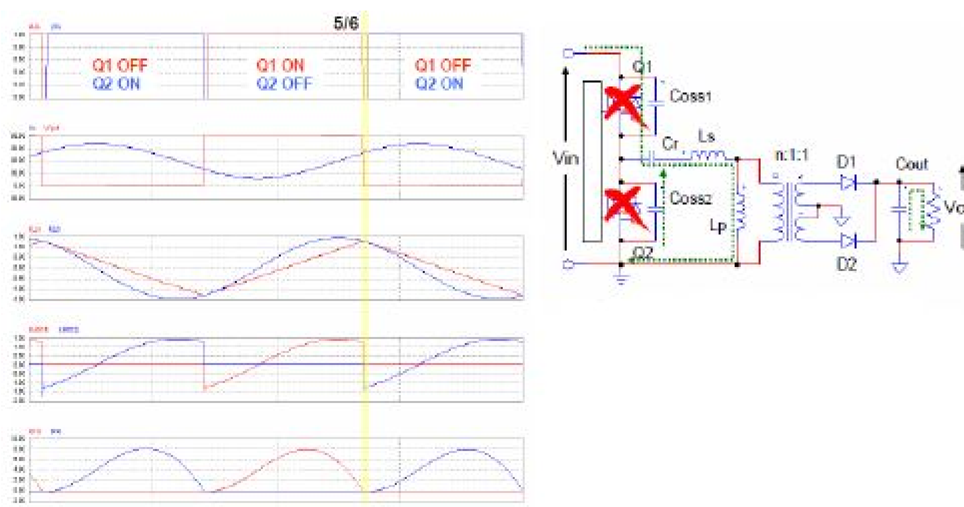

Figure 35: LLC Converter Working Principle for phase 5[29]

In Phase 6, Q1 is in turn-off and Q2 is in turn-on. The stored energy in the resonant circuit is transferred to the secondary side. Phase 6 is ended when the resonant current Ir drops to zero.

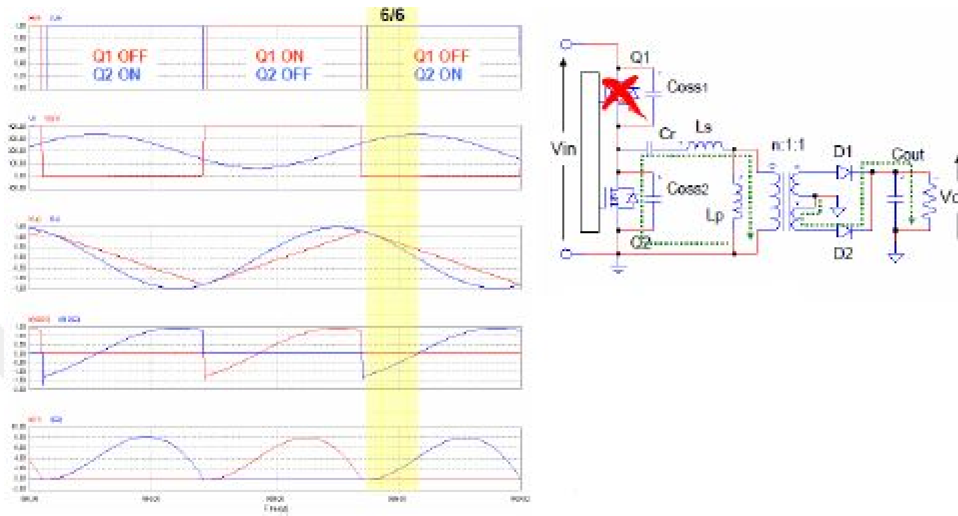

Figure 36: LLC Converter Working Principle for phase 6[29]

3.4.2 AC equivalent circuit

The only fundamental voltage and current are used because of the filtering characteristic of the resonant network. It should be assumed that only the fundamental component transfer the energy to the secondary side to compute alternating current(AC) equivalent circuit and AC resistance. AC current source is connected to the input of the secondary rectifier to calculate the AC resistance as shown in Fig. 37.

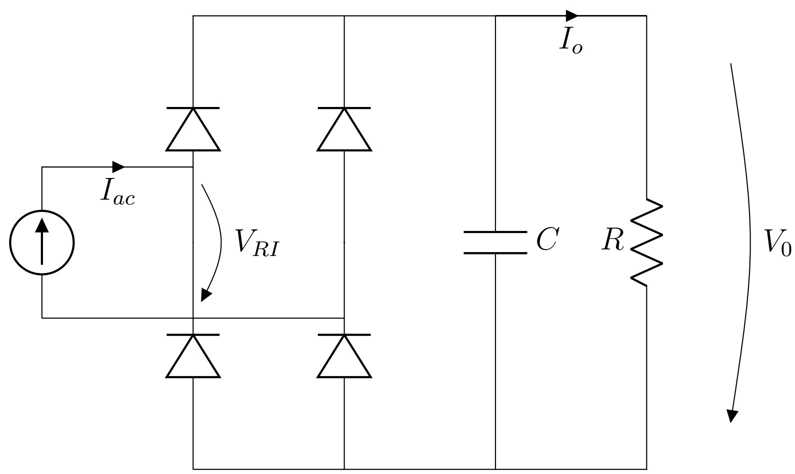

Figure 37: AC equavialent circuit for LLC converter

The I_{ac} is obtained as in Eq.(13).

$$I_{ac} = \frac{\pi.Io}{2} sin(wt) \tag{13}$$

The rectifier input of the circuit is replaced with a current generator to perform AC analysis. A square voltage wave appears on the VRI points. The fundamental component of input voltage can be calculated as;

$$V_{RI} = +V_0 \quad if \ sin(wt) > 0 \tag{14}$$

$$V_{RI} = -V_0 \quad if \ sin(wt) < 0 \tag{15}$$

$$V_{RI}^F = \frac{4.Vo}{\pi} sin(wt) \tag{16}$$

AC equivalent circuit on the primary side is demonstrated in Fig.38.

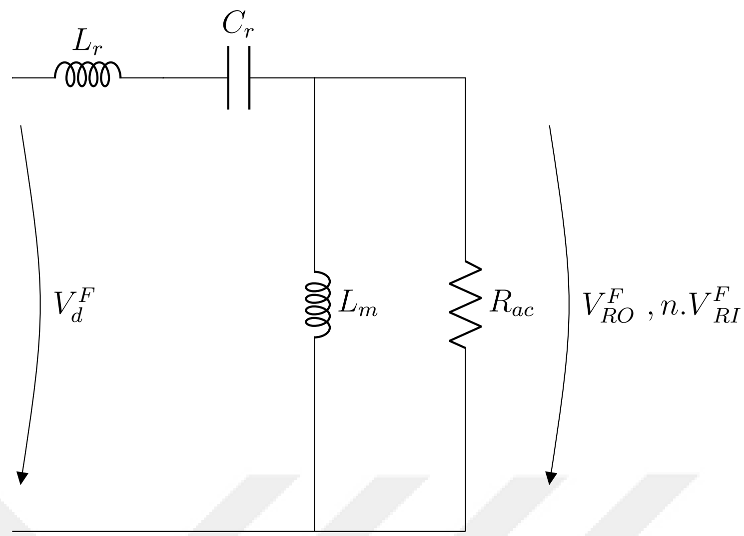

Figure 38: AC equavialent circuit for LLC converter

The voltage gain is obtained from the equivalent circuit;

$$M = \frac{V_{RO}^F}{V_d^F} = \frac{n.V_{RI}^F}{V_d^F} = \frac{\frac{4n.V_0}{\pi} sin(wt)}{\frac{4.V_{in}}{\pi.2} sin(wt)} \tag{17}$$

$$M = M_V = \sqrt{\frac{L_p}{L_p - L_r}} = \sqrt{\frac{m}{m-1}} \quad if\ w = w_0 \tag{18}$$

AC equivalent resistance is calculated by using only fundamental components. AC resistance is given as Eq.(19).

$$R_{ac} = \frac{V_{RI}^F}{I_{ac}^F} = \frac{V_{RI}^F}{I_{ac}} = \frac{8.V_0}{\pi^2.I_0} = \frac{8}{\pi^2} R_0 \tag{19}$$

This equation gives that the load is reflected from the secondary side to the primary side of the transformer.

Since there are two inductances and one capacitance in LLC resonant converter, there are two resonant frequencies. w_o frequency is only between L_r and C_r as Eq.(20). The other resonant frequency is between L_m and L_r as Eq.(21).

$$w_0 = \frac{1}{\sqrt{L_r.C_r}} \tag{20}$$

$$w_p = \frac{1}{\sqrt{L_p.C_r}} \quad where\ L_p = L_m + L_r \tag{21}$$

3.4.3 Quality Factor and Frequency-Gain Graph

The quality factor, Q, is the parameter that describes how quickly the resonance gain falls from the resonant frequency when the load is changed. The calculation of quality factor is in Eq.(22). Q affects the voltage gain greatly. In an LLC resonant circuit design, Q needs to be controlled within a certain range so that the voltage stress is minimized on the resonance inductor or resonant capacitor. When the quality factor is increased, the bandwidth is decreased.

$$Q = \sqrt{\frac{L_r}{C_r}}\frac{1}{R_{ac}} \tag{22}$$

The quality factor is the ratio of the stored energy to the dissipated energy in a period. Increasing the quality factor causes a decrease in bandwidth. It is not a fixed parameter. It changes proportionally to the load. As the quality factor changes, the gain curve also changes. Thus the gain curve changes when the load changes. The gain graphs corresponding to all loads are almost the same at the resonant frequency, so it is preferable to work around the resonant frequency as shown in Fig.39[30].

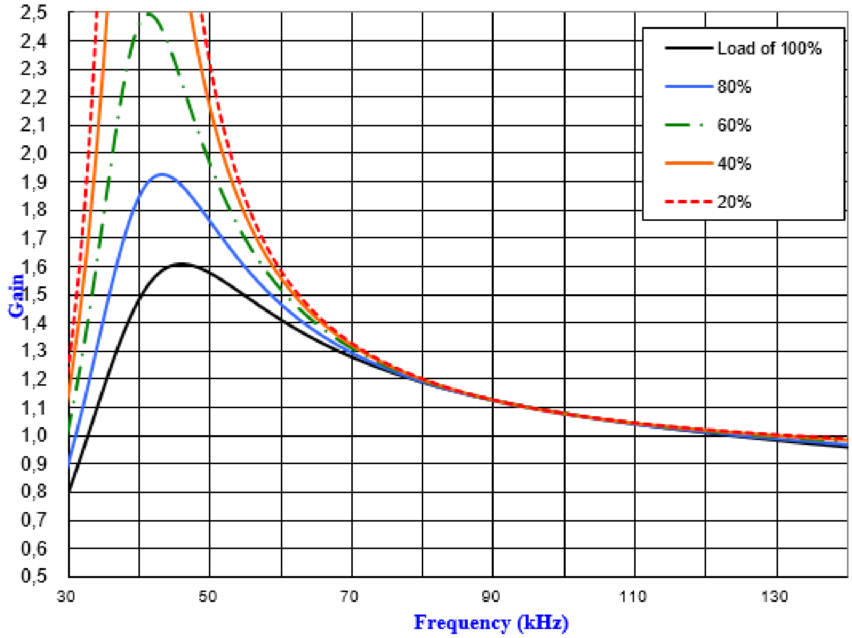

Figure 39: Voltage Gain versus frequency graph with different loads

The m value is the ratio of the magnetizing inductance to the resonant inductance as demonstrated in Fig.40. The lower m value allows reaching higher gain points. In higher gain, the controlled frequency range is narrower. There may be an unstable regulation at very high gain points. When the m value is decreased, the circulating current and switching losses increase in the primary. Higher m values have higher magnetizing inductance. Lower magnetizing current and high efficiency can be achieved with a higher m value.

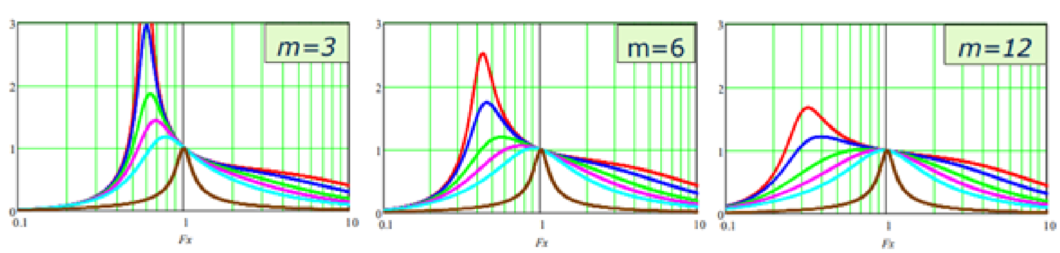

Figure 40: Gain graph according to different m value[30]

3.4.4 Working Regions of LLC Resonant Converter

There are two working regions for LLC resonant converter as shown in Fig.41. The left of the max gain point is called the capacitive zone. Ip(IR) current leads with respect to the voltage. Therefore this area is called a capacitive region. In the region, high negative voltage spikes occur. When operating is in the capacitive zone, the diode of MOSFET goes into reverse recovery during the switching transition and causes serious noise and losses. Another problem is that output voltage is out of control due to the reversed gain slope.

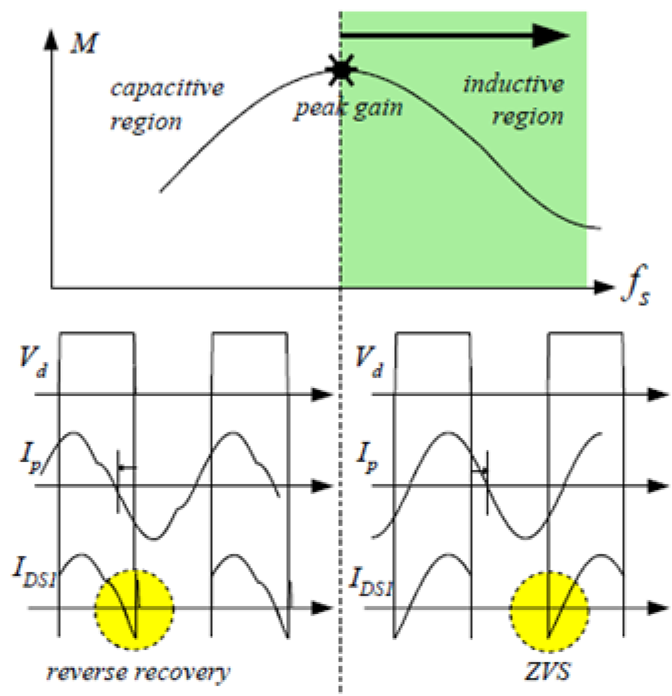

Figure 41: Capacitive and Induktive Region[30]

The right of the max gain point is called the inductive zone. The resonant current lags the resonant voltage, so this region is called the inductive region. ZVS is achieved in this region. It prevents capacitive losses and enables more efficient designs.

3.4.4.1 *Switching frequency equal to resonant frequency*

The working frequency regions in the inductive zone are shown in Fig.42.

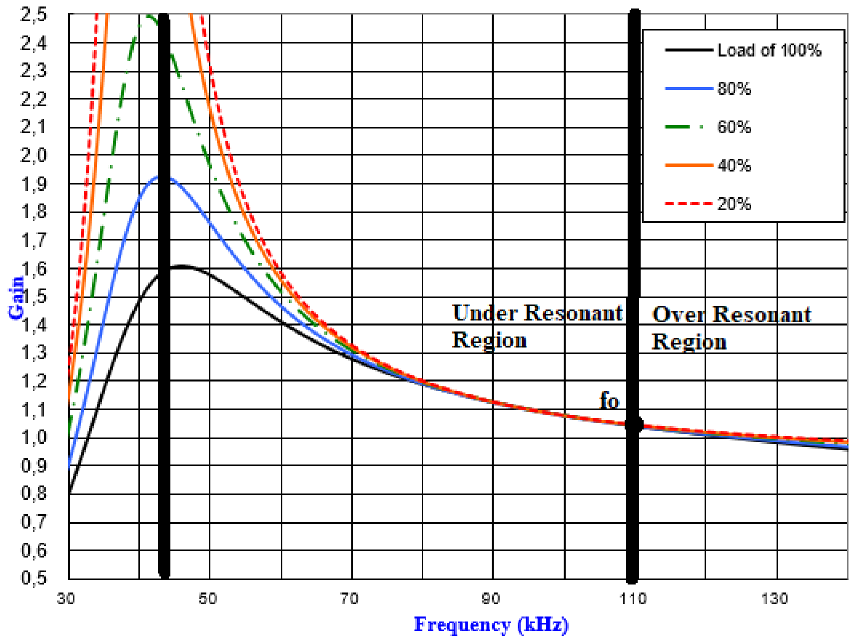

Figure 42: Under resonant and over resonant regions

The switching frequency is the same as the resonant frequency between L_r and C_r. Each half of the switching period includes full power transfer. Q_1 and Q_2 have switched on alternately. Resonant tank gain is equal to one. LLC resonant converter has the best-optimized efficiency. Therefore, the transformer winding ratio is designed to operate at nominal input and output voltages at this point.

3.4.4.2 *Switching frequency larger than resonant frequency*

This area is called an over resonant frequency zone. The circulating current in the primary is low and the transmission losses are also low due to the low circulating current. Secondary diodes have reverse recovery losses. EMI performance is poor compared to the under resonant. Its frequency range is wide and can be controlled easily. In a no-load condition, the switching frequency increases very high. For this problem, the frequency limitation or burst mode operation is used. It is preferred in applications where a low output voltage is required such as LCD TV applications, laptop adapter applications, etc.

3.4.4.3 Switching frequency smaller than resonant frequency

The circulating current in the primary is high and the primary loss is greater. There is no reverse recovery loss in secondary diodes. Operating below resonance has a narrow frequency range with respect to load change. Because the frequency is limited not to enter the capacitive region. It is generally preferred for high output voltage applications.

3.4.5 Design of LLC resonant converter

FA6A30 LLC resonant IC is used as LLC resonant controller. The LLC resonant controller drives two MOSFETs with a 50 percent duty cycle. MOSFETs work in opposite phases to each other. There is a certain amount of dead time between two MOSFETs. Deadtime is set automatically to prevent signal transitions and hard switching[31]. The controller has a high-voltage start-up pin. A high-voltage (HV) start-up circuit in IC enables smaller card design and lower power consumption. The controller has over current, overload, over-voltage, and overheat protection[31]. The block diagram of resonant controller IC is shown in appendix Fig.78.

At the start-up time, the HV start-up circuit in IC is active for a certain time until Vcc voltage is obtained. The Vcc voltage is generated by the auxiliary winding on the transformer. When AC is first turned on, the startup circuit is activated until the Vcc voltage reaches a certain level. When Vcc is reached to 13v, the soft start block is activated and it starts switching the MOSFETs. The Switching continues until the Vcc voltage reaches 9V when AC is reversed to turn-off state. During this time, a certain amount of energy in bulk capacitors is transferred to the secondary. An extra separate topology is not needed to generate Vcc voltage with the HV start-up circuit.

The waveform at startup time is shown in Fig.43.

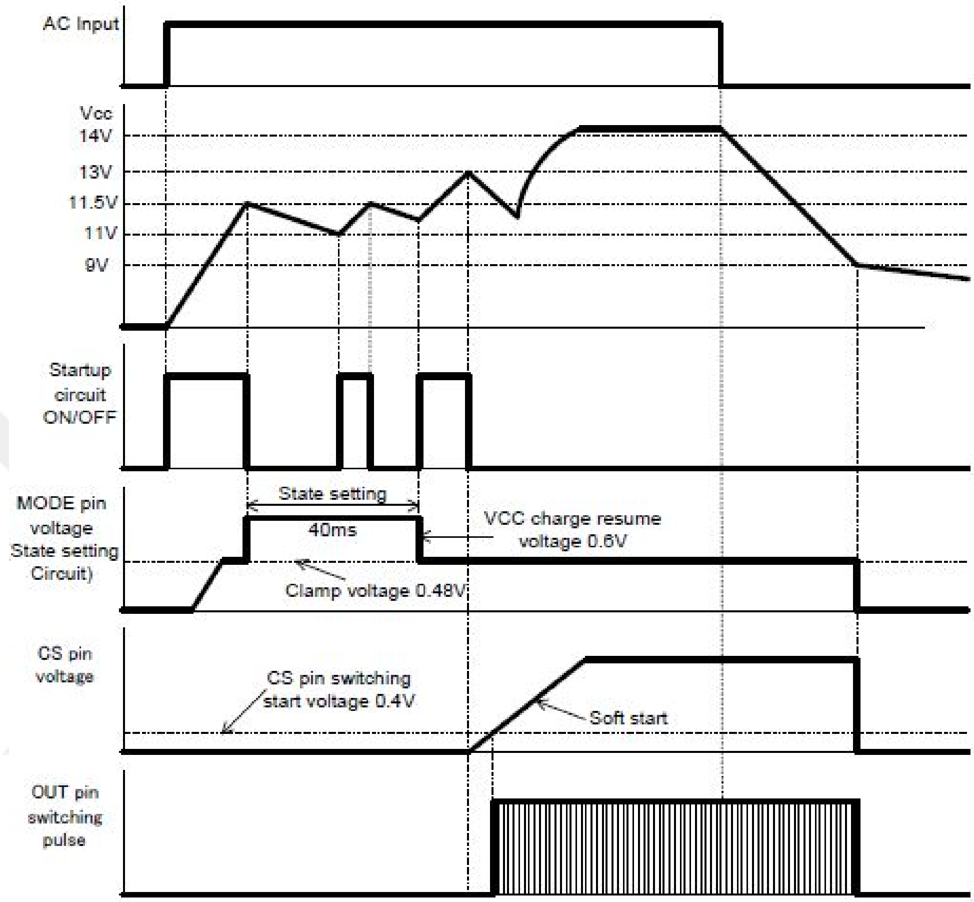

Figure 43: Startup waveforms of controller[31]

A_e value is 81.80 mm^2, B_m value is about 500 mT for EFD core. By using Eq.(23), the value of N_s is determined as 6. The total leakage inductance is 140 uH, the magnetizing inductance is 660 uH for EFD type transformer. The primary side of the two transformers is connected in series and the secondary side of transformers is connected in parallel. The suitable resonant capacitor is selected for 110kHz operation frequency by using Eq.(26).

A_e value is 97mm2, B_m value is 390 mT for the toroidal core. By using Eq.(23), the value of N_s is determined as 5. By using Eq.(24), the N_p value is determined as 42. For toroidal transformer, the leakage inductance is measured as a maximum of

10 uH and the magnetizing inductance is 2 mH. 55uH coil is connected externally in series for resonant inductance. The suitable resonant capacitor is selected for 110kHz operation frequency by using Eq.(26).

$$N_s = \frac{(V_o + V_f).T_{on}}{2.A_e B_m} \tag{23}$$

$$n = \frac{N_p}{N_s} \geq \frac{V_{in}}{2.(V_o + V_f)} \tag{24}$$

$$N_p = N_s.n \tag{25}$$

$$f_0 = \frac{1}{2\pi\sqrt{L_r.C_r}} \tag{26}$$

$$f_p = \frac{1}{2\pi\sqrt{L_p.C_r}} \quad where\ L_p = L_m + L_r \tag{27}$$

The circuit diagram is shown in Fig.44. A toroidal transformer and resonant coil are used externally in series. In another study, two EFD type transformers were used in LLC resonant stage. The performance of two EFD type transformers and a toroidal transformer will be compared in the chapter of experimental results. A turn-off circuit is put in the design for two MOSFETs. The turn-off circuit provides faster closing of the MOSFET and reduces switching losses. Vcc voltage is generated by the auxiliary winding on the transformer and used as the supply voltage for the controllers.

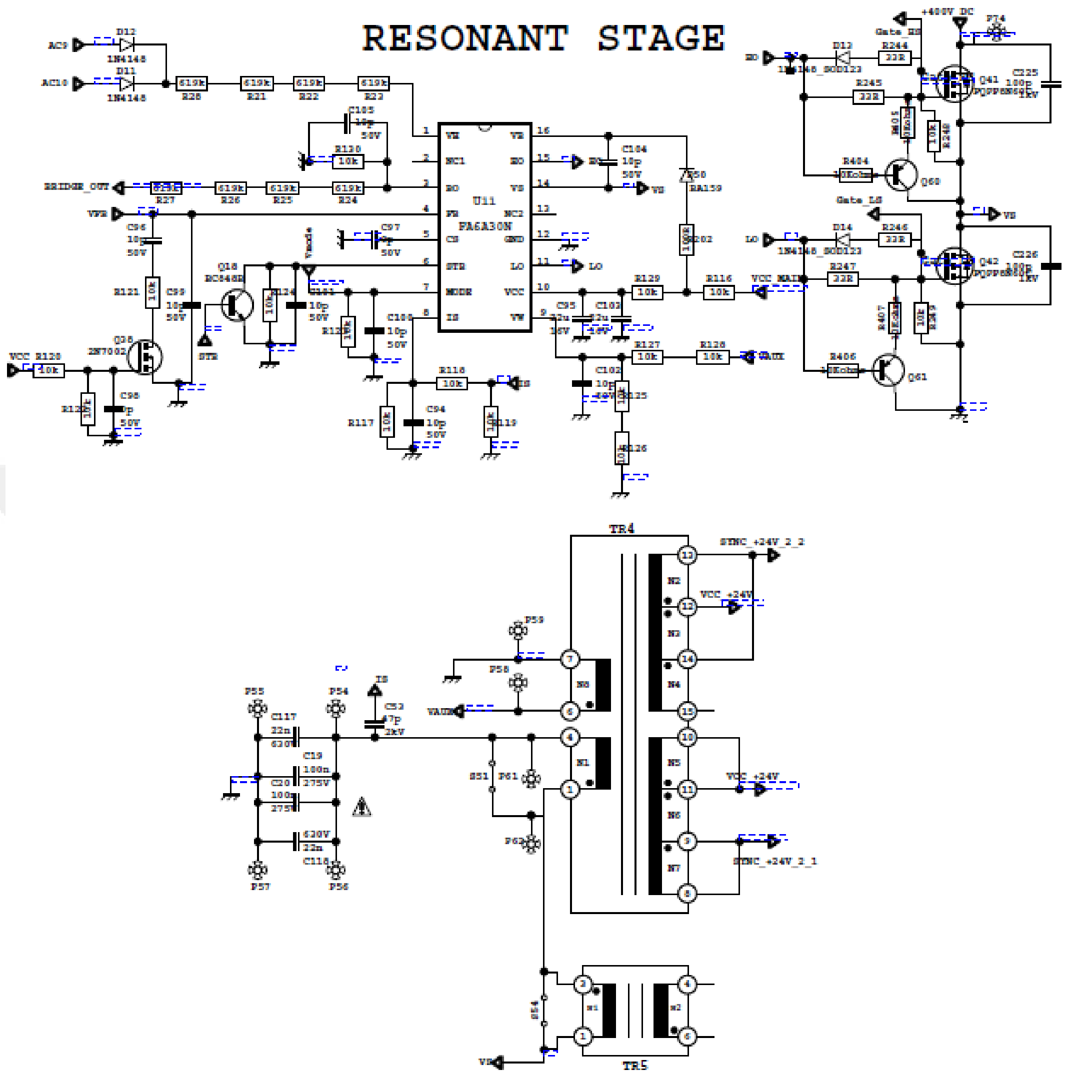

Figure 44: Circuit schema of LLC resonant converter

3.5 *Transformations of Half Bridge LLC Converter*

3.5.1 Integrated Transformer

For the LLC resonant converter, a resonant inductance and a magnetizing inductance are integrated into the same transformer, which is called the integrated power transformer. The leakage of the transformer is used a resonant inductance. EFD 50/56 type integrated transformer was used in this study. The electrical and mechanical parameters are depicted in Tab.2. The effective magnetic path is 119.3mm, the effective cross-sectional area is 81.80 mm^2, the effective volume is 9765 mm^3, the dimension of the transformer is 50/56/12 mm. The maximum height is 12 mm and the other components which have 12mm maximum height was selected in hardware design. The power supply unit has a 12 mm maximum component height with EFD 50/56 transformer for a slim design.

Table 2: Electrical and mechanical parameters for EFD 50/56 type transformer

	$1xEFD50/56$
Effective magnetic path length(Le)	119.3 mm
Effective cross sectional area(Ae)	81.80 mm^2
Effective volume(Ve)	9765 mm^3
Dimension of transformer	50/56/12 mm

There are different core parameters for each core type. The core type of power transformer and line filter is different from each other. So the suitable core type is selected for the design. The core loss is decreased when the temperature is increasing on the core. The minimum core loss is in 100°. So, the maximum working temperature is determined between 100°-105°. The initial permeability is relative permeability in low magnetic flux density. The temperature versus initial permeability is shown in Fig.45.

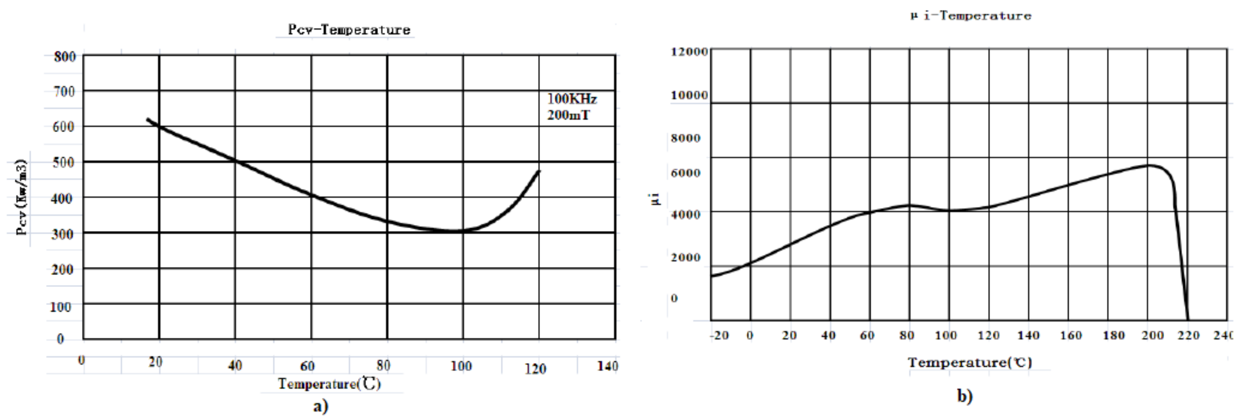

Figure 45: a)Graph of core loss vs temperature b)Graph of initial permeability vs temperature for EFD5056 Core

3.5.2 Toroidal Transformer

A toroidal transformer is a type of power transformer. The toroidal transformer has a distributed air gap on the surface of the core. So, the air gap is not set externally by the designer. In this design, the leakage inductance of the transformer is set as small as possible. The ER3010 coil was used as resonant ınductance. The electrical and mechanical parameter of toroidal transformer is depicted in Tab.3. The effective magnetic path is 110.4 mm, the effective cross-sectional area is 97.4 mm^2, the effective volume of core is 10767 mm^3. This parameter is so close to EFD 50/56 type transformer. So, the two transformers can be compared. The mechanical dimension of the core is 47/27/10 mm. The core maximum height is 10 mm but the maximum height will be 15 mm with the copper height. So, the maximum component height is 15 mm for the power supply unit with the toroidal transformer.

When the switching frequency is increased, the core loss increase. The graphs of core loss and initial permeability versus temperature are shown in Fig.46.

Table 3: Electrical and mechanical parameters for toroidal type transformer

	$1xToroidal47/27/10$
Effective magnetic path length(Le)	110.4 mm
Effective cross sectional area(Ae)	97.4 mm^2
Effective volume(Ve)	10767 mm^3
Dimension of transformer	47/27/10 mm

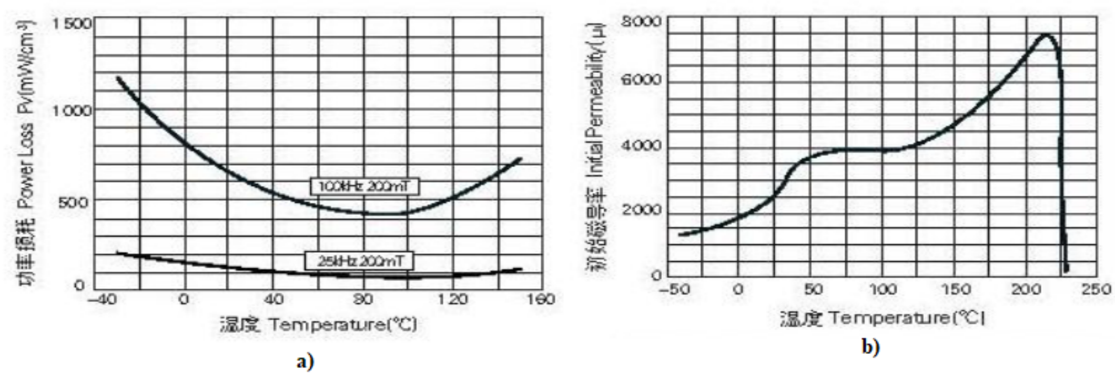

Figure 46: a)Graph of core loss vs temperature b)Graph of initial permeability vs temperature for Toroidal Core

The working frequency is around 100kHz so the minimum core loss is 500 mW/cm^3 for the toroidal transformer. For the core of the EFD 50/56 type transformer, the core minimum core loss is 300 mW/cm^3. The initial permeability versus temperature graph is almost the same until 100° for two type cores.

CHAPTER IV

RESULTS

4.1 Simulation Results for LLC Resonant Converter

A simulation study was done for LLC resonant converter by using MATLAB Simulink program as shown in Fig.47. The input voltage is 390VDC and the Output power is 384W in 24V@16A. Resonant parameters were calculated as Lr: 140uH, Cr: 15nF, Lm: 660uH. The resonant frequency was calculated as 110kHz with determined parameters. The operating frequency is set at 110kHz. Secondary output diodes are designed in a center-tapped structure. The output capacitor is determined as 4000uF to obtain the optimum output voltage ripple level. Coils and capacitors were simulated with their series resistance value.

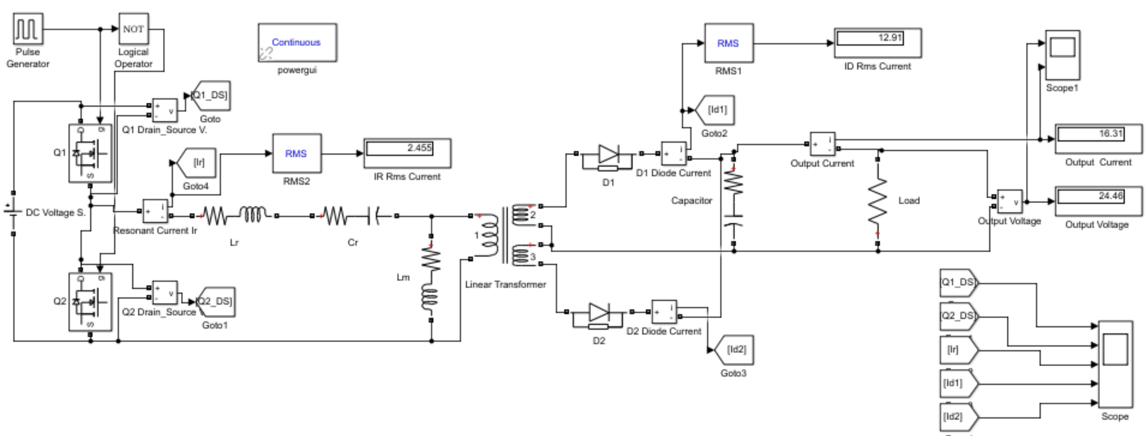

Figure 47: Simulation circuit for LLC resonant converter

The waveforms are obtained at the end of the simulation as shown in Fig.48. Q1 and Q2 switching elements are determined as MOSFET to operate at high frequencies. MOSFETs switch at different times with a 50 percent duty cycle. In the simulation, the switchings of the MOSFETs are taken ideally and there is no dead time between two MOSFETs. In the hardware application, there is a certain dead time for the MOSFETs to prevent short circuits and to make healthy switching. In turn-on times, the switching elements are switched on with the zero voltage switching (ZVS) method.

The resonant current is very close to the sinus signal. Because the resonant frequency and switching frequency are equal to each other. If these frequencies are removed from each other, distortions will occur in the resonant current. The peak value of the resonant current was obtained as 3.4A and the RMS current is 2.45A. Secondary side rectifier diodes waveforms are depicted also in Fig.48. When the D1 diode is activated in a positive cycle, the D2 diode is activated in a negative cycle to supply the load. The peak current value passing through each diode was simulated as 26A and RMS current is 12.91A. Diodes are turned on with the frequency of the primary side switching elements.

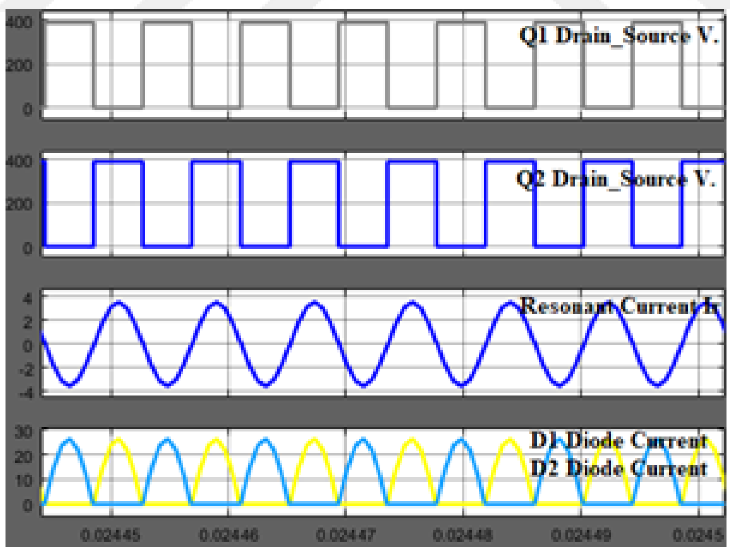

Figure 48: Waveforms for LLC resonant converter

The waveforms of the output voltage and current are shown in Fig.49. The output voltage value is 24.46V, the output current is 16.31A. It reaches the steady-state point after 2ms with a small overshoot at startup time.

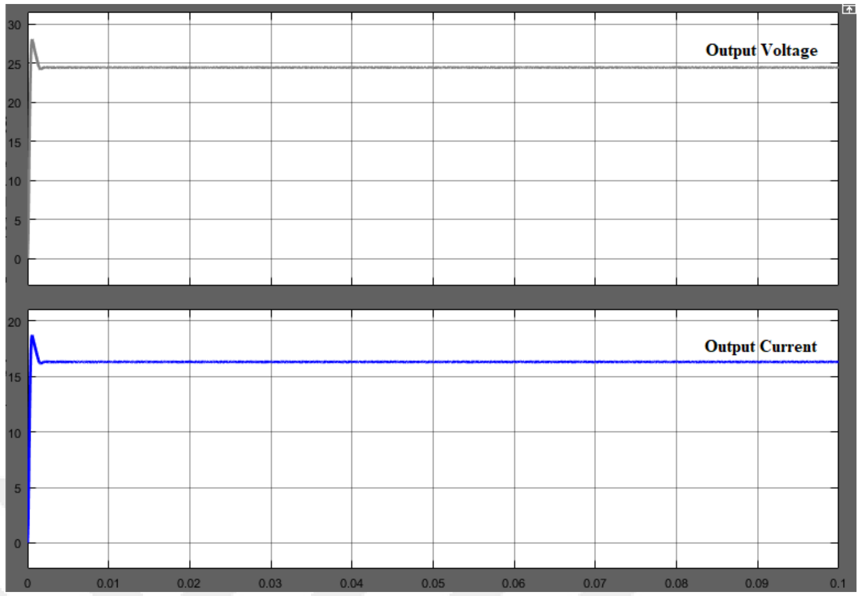

Figure 49: Output voltage and output current waveforms

The overshoot graph and ripple graph of the output voltage are shown in Fig.50. Output voltage settles in steady-state after 2ms in the start-up time. The output ripple value is around 30mV. Choosing a smaller value output capacitor is increased the ripple voltage. The output ripple can be allowed up to a certain level. The equivalent series resistance(ESR) and equivalent series inductance(ESL) values of the capacitor are also effective in the output ripple value.

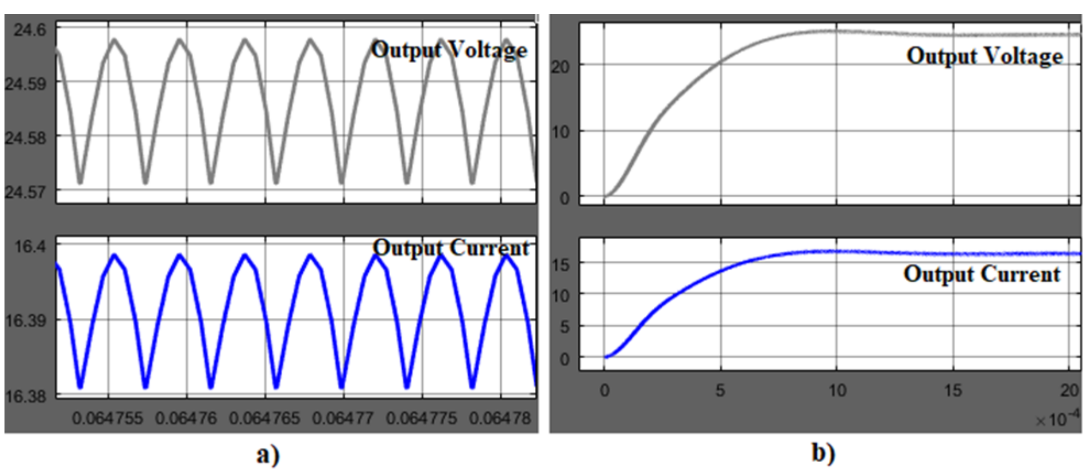

Figure 50: a)Ripple value of output voltage b)Output Voltage Overshoot

The resonant frequency and operating frequency were worked at 110 kHz. the waveform results were obtained with the determined resonant parameters. Output voltage and output current ripple values are within the specified limit. Current stress is high on the output diodes. The synchronous rectifier is used in the hardware design to prevent overheating and losses.

4.2 Experimental Verification of PFC Stage

The coil current and gate-source voltages are shown in Fig.51 for the PFC stage.PFC stage is controlled with a 180° phase shift between two branches.

Figure 51: Gate voltages of MOSFETs and coil current at PFC stage

-Channel 1(Yellow): The Coil Current

-Channel 2(Blue) : Gate to Source Voltage of MOSFET for a branch

-Channel 3(Purple): Gate to Source Voltage of MOSFET for another branch

The coil current and PFC input voltage are demonstrated as a general waveform in Fig.52. The current peak is about 7.4A at 100VAC.100 VAC voltage is the most stressful voltage point for the PFC stage in this study. When the voltage is decreased, the current and thermal stress is increased.

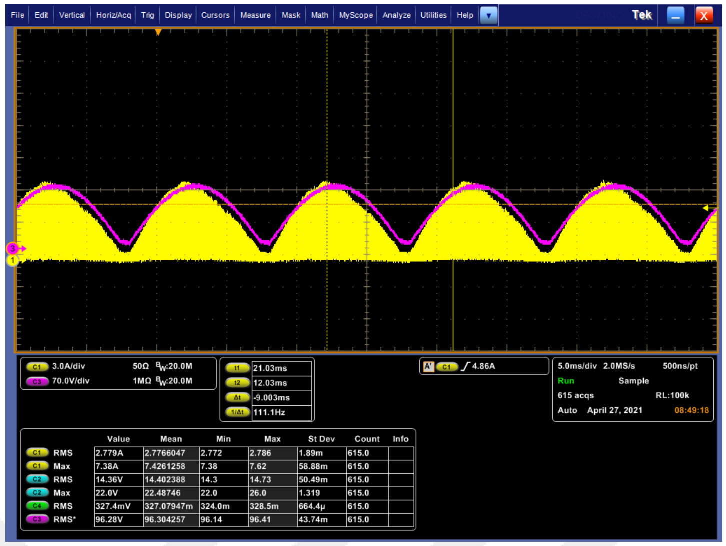

Figure 52: PFC input voltage and coil current at 100VAC

-Channel 1(Yellow) : The Coil Current at 100VAC

-Channel 3(Purple) : PFC Input Voltage at 100VAC

The coil current and PFC input voltage are demonstrated for 220VAC input voltage in Fig.53. The coil current is about 3.6A.

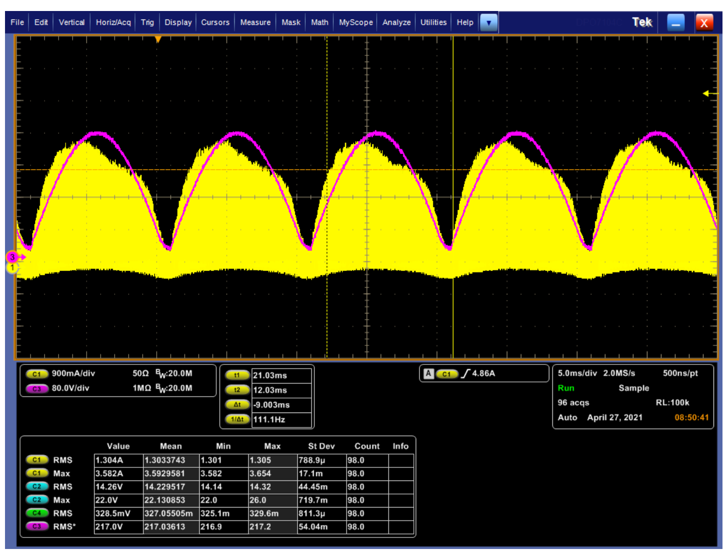

Figure 53: PFC input voltage and coil current at 220VAC

-Channel 1(Yellow) : The Coil Current at 220VAC

-Channel 3(Purple) : PFC Input Voltage at 220VAC

The maximum gate-source voltage is 20V for each branch. The gate-source voltage and coil current are shown in Fig.54.

Figure 54: PFC gate voltage and coil current for a branch

-Channel 1(Yellow) : The Coil Current

-Channel 3(Purple) : Gate to Source Voltage of MOSFET for a branch

For the other branch, the gate-source voltage and coil current are shown as in Fig.55. Gate-source voltages are similar to each other.

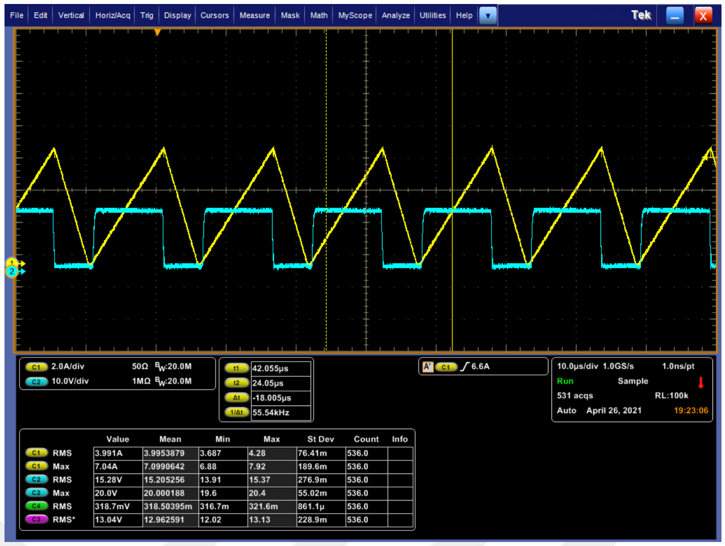

Figure 55: PFC gate voltage and coil current for other branch

-Channel 1(Yellow) : The Coil Current

-Channel 2(Blue) : Gate to Source Voltage of MOSFET for another branch

PFC stage runs the discontinuous mode for 220VAC input voltage. The controller detects the core reset of the inductor and valley points of MOSFET. The drain-source voltage and coil current are demonstrated as in Fig.56.

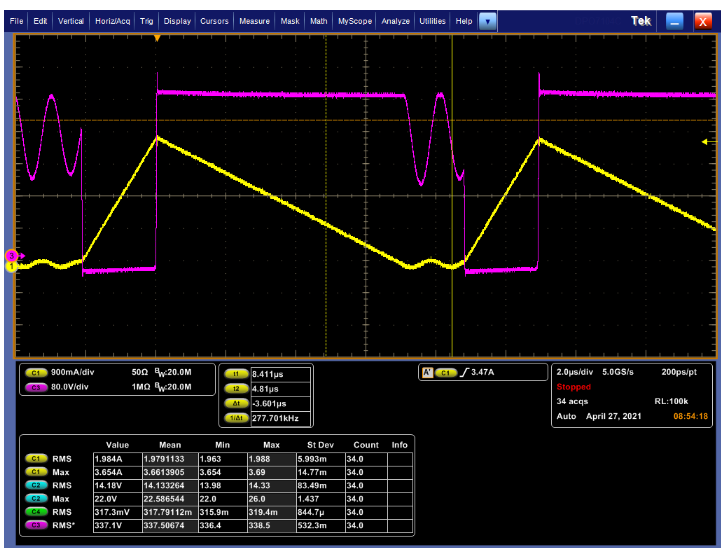

Figure 56: PFC MOSFET drain voltage and coil current at 220VAC

-Channel 1(Yellow) : The Coil Current

-Channel 3(Purple) : Drain to Source Voltage of MOSFET at 220VAC

PFC stage runs the critical conduction mode for 100VAC input voltage. The drain-source voltage and coil current are demonstrated as in Fig.57 at 100VAC.

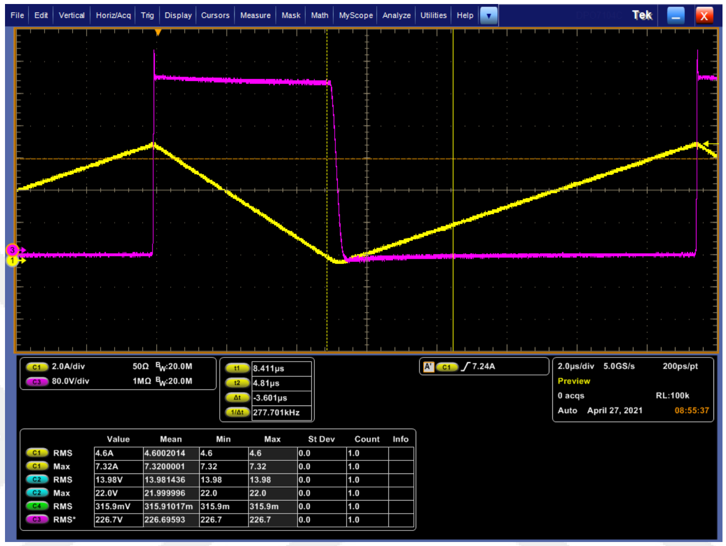

Figure 57: PFC MOSFET drain voltage and coil current at 100VAC

-Channel 1(Yellow) : The Coil Current

-Channel 3(Purple) : Drain to Source Voltage of MOSFET at 100VAC

PFC input voltage is the output of the full-wave rectifier. The signal is not DC voltage. The frequency is changed in the level of different PFC input voltages. The frequency is about 65kHz at the peak point of coil current as shown in Fig.58.

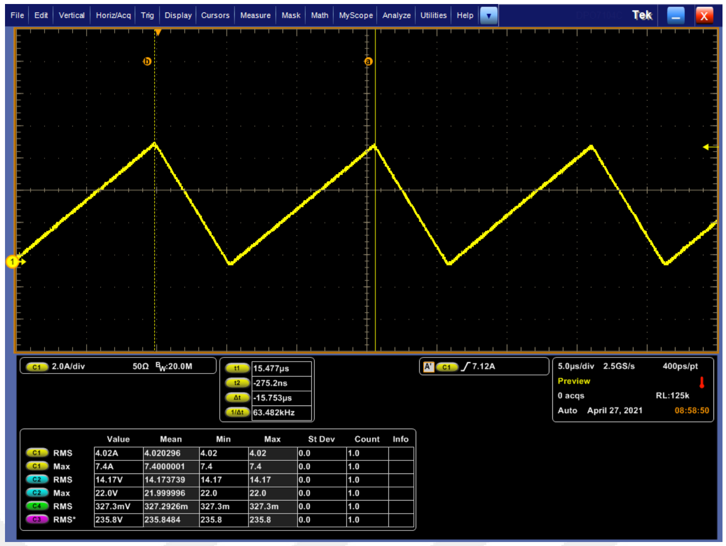

Figure 58: Coil current at peak point

-Channel 1(Yellow) : Peak level of the coil current

The frequency is increased at the breaking point of the coil current. The frequency is about 102 kHz at the breaking point ofcoil current as shown in Fig.59.

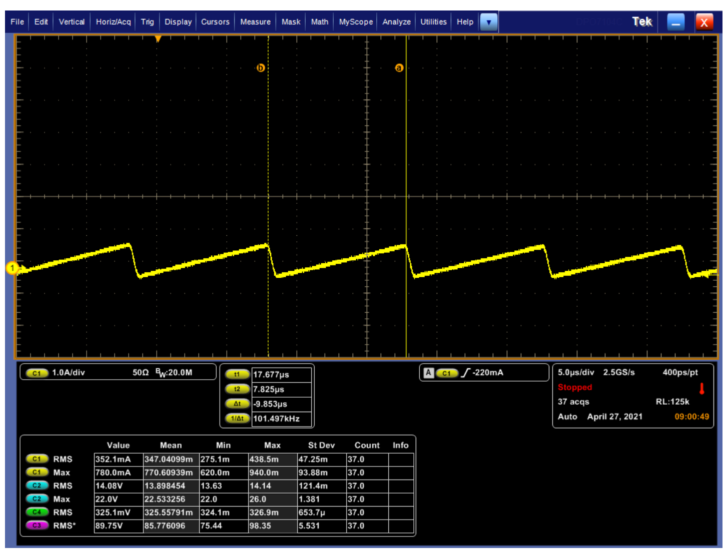

Figure 59: Coil current at break point

-Channel 1(Yellow) : Breaking level of the coil current

4.3 Experimental Verification of LLC Stage

Resonant current and gate signals are shown in Fig.60 at full load. The switching frequency is around 105 kHz. The switching frequency is close to the resonant frequency. Switching elements operate at a 50% duty cycle with a certain dead time. The resonant current is close to the sinus signal.

Figure 60: Gate voltages of MOSFETs and resonant tank current for LLC stage

-Channel 1(Yellow) : The Resonant Tank Current

-Channel 2(Blue) : Gate to Source Voltage of MOSFET Q2

-Channel 3(Purple) : Gate to Ground Voltage of MOSFET Q1

The soft-starting waveforms are depicted in Fig.61. When AC input is on, Vcc voltage is generated to activate the switching. After the V_{cc} voltage is generated, the soft-start operation is started.

Figure 61: Soft-starting waveforms

-Channel 1(Yellow) : Gate to Source Voltage of MOSFET Q1

-Channel 2(Blue)   : Output Voltage

-Channel 3(Purple) : Gate to Ground Voltage of MOSFET Q2

The soft-start is shown clearly on output waveforms in Fig.62. The soft-start time is about 40ms, then the voltage is regulated at 24VDC.

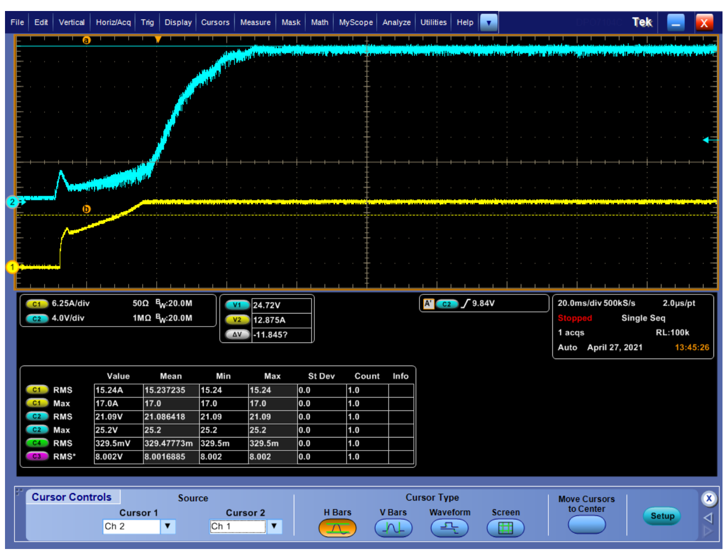

Figure 62: Soft-starting for output waveforms

-Channel 1(Yellow) : Output Current

-Channel 2(Blue) : Output Voltage

ZVS is clearly shown in Fig.63. Firstly, the drain voltage of the Q2 MOSFET decreases to zero. Switching occurs after a certain dead time. ZVS significantly reduces the loss of switching.

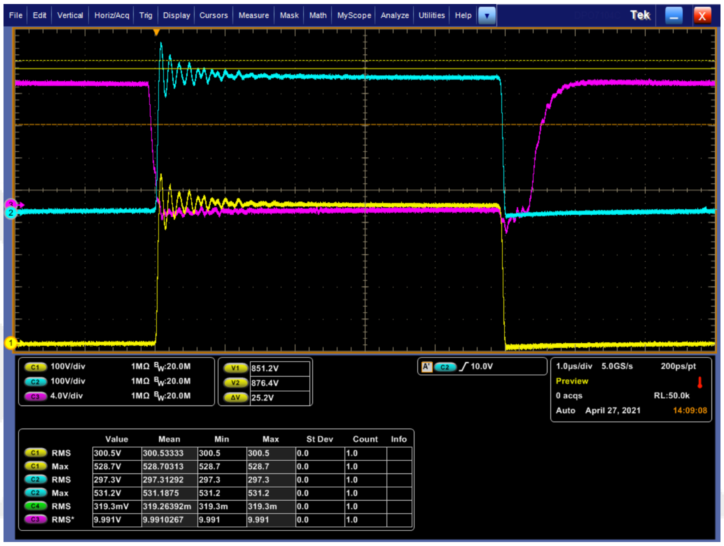

Figure 63: ZVS for low side Q2 MOSFET

-Channel 1(Yellow) : Gate to Source Voltage of MOSFET Q1

-Channel 2(Blue) : Drain to Source Voltage of MOSFET Q2

-Channel 3(Purple) : Gate to Ground Voltage of MOSFET Q2

The switching frequency is changed between 99 kHz-105 kHz, which is called fitter. The fitter provides to reduce EMI noises as shown in Fig.64.

Figure 64: The fitter for the resonant tank current

-Channel 1(Yellow) : The Resonant Tank Current in the fitter

In the no-load state, the switching occurs as packages at 115Hz. This working condition is called burst mode as shown in Fig.65. In burst mode, the transmission and switching losses are highly reduced. Thus, power consumption drops to a certain level.

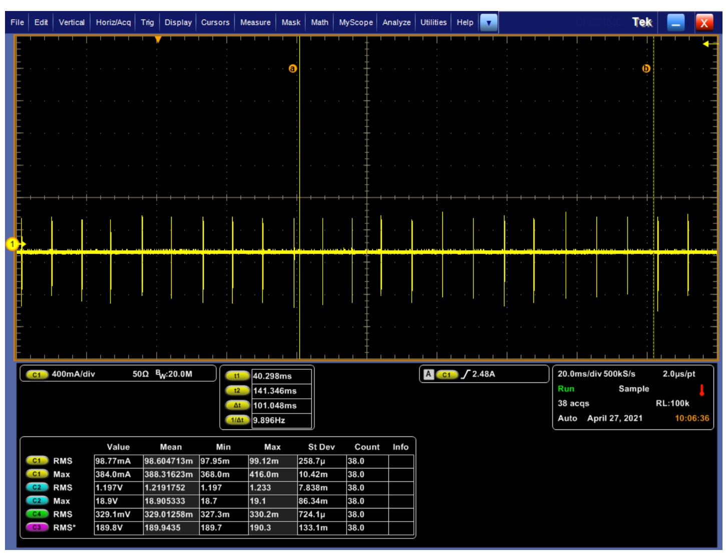

Figure 65: The resonant tank current at no load

-Channel 1(Yellow) : The Resonant Tank Current at no-load

The gate and drain voltages of the MOSFET are shown in Fig.66 for the synchronous rectifier. First of all, current passes through the body diode of the MOSFET. When the body diode is active, the gate voltage is increased and the current flows through the Rds-on of MOSFET.

Figure 66: Gate and drain voltage for MOSFET of synchronous rectifier

-Channel 2(Blue) : Drain to Source Voltage of Synchronous MOSFET

-Channel 3(Purple) : Gate to Source Voltage of Synchronous MOSFET

The drain-source voltage and rectifier current is demonstrated in Fig.67. The switching frequency of the rectifier stage is the same as LLC resonant switching frequency.

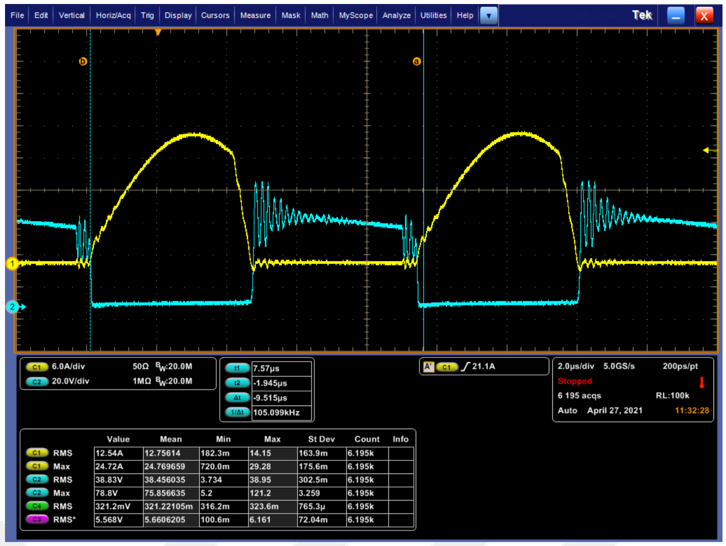

Figure 67: Drain-source voltage and drain current for MOSFET of the synchronous rectifier

-Channel 1(Yellow) : Current of Synchronous MOSFET at a cycle

-Channel 2(Blue) : Drain to Source Voltage of Synchronous MOSFET

The currents of synchronous rectifier which have positive and negative cycles are depicted in Fig.68. The maximum peak current is 24A for a cycle, the maximum peak current is about 23A for another cycle. The two-ampere difference may occur due to the layout and the location of synchronous MOSFET. This difference is within the acceptable limit.

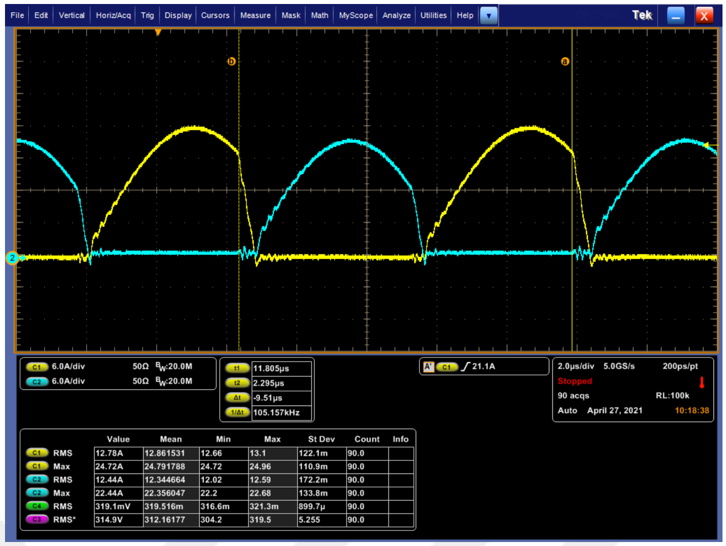

Figure 68: The current of synchronous rectifier for two cycles

-Channel 1(Yellow) : Current of Synchronous MOSFET for a cycle

-Channel 2(Blue) : Current of Synchronous MOSFET for another cycle

The primary resonant tank current and synchronous rectifier current for a cycle are shown in Fig.69.

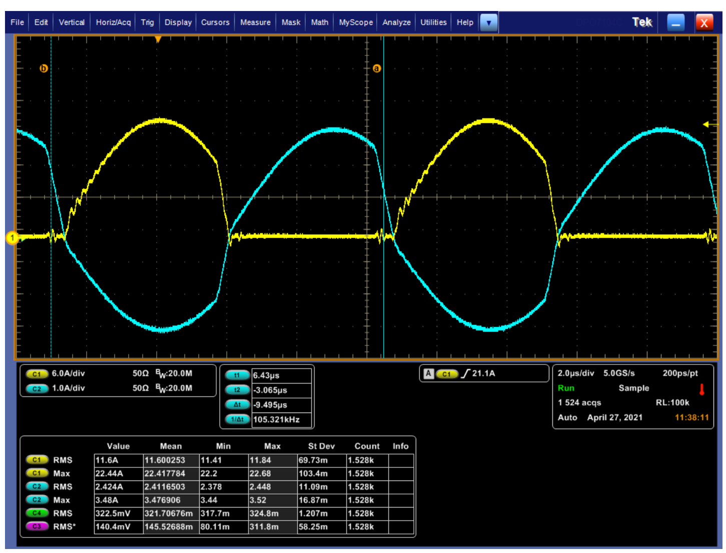

Figure 69: The resonant tank current and synchronous rectifier current

-Channel 1(Yellow) : Current of Synchronous MOSFET for a cycle

-Channel 2(Blue)   : The Resonant Tank Current

The dynamic response of the converter is demonstrated as in Fig.70 during the changing of load which is from full load to no-load and vice versa.

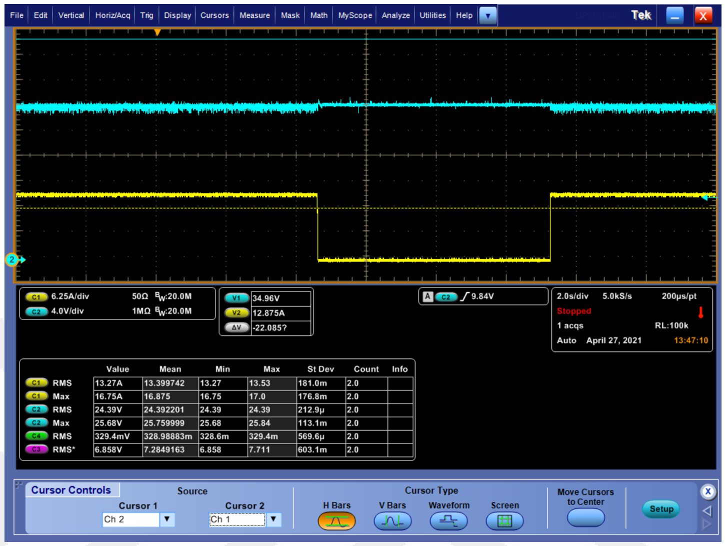

Figure 70: The dynamic response for the output voltage and current

-Channel 1(Yellow) : Output Current

-Channel 2(Blue)   : Output Voltage

The output ripple voltage is measured as 200mV at full load condition as depicted in Fig.71. High switching frequency affects the output voltage and creates spikes on the output voltage. So, these spikes are neglected.

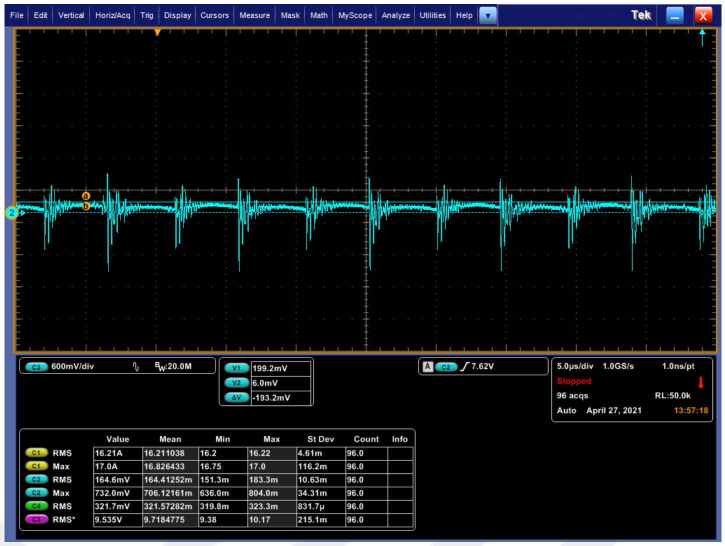

Figure 71: The output ripple voltage

-Channel 2(Blue) : Output Voltage

The output ripple current is measured about 500mA at full load condition as shown in Fig.72. The ripple current ratio is at about 3% according to the full load current.

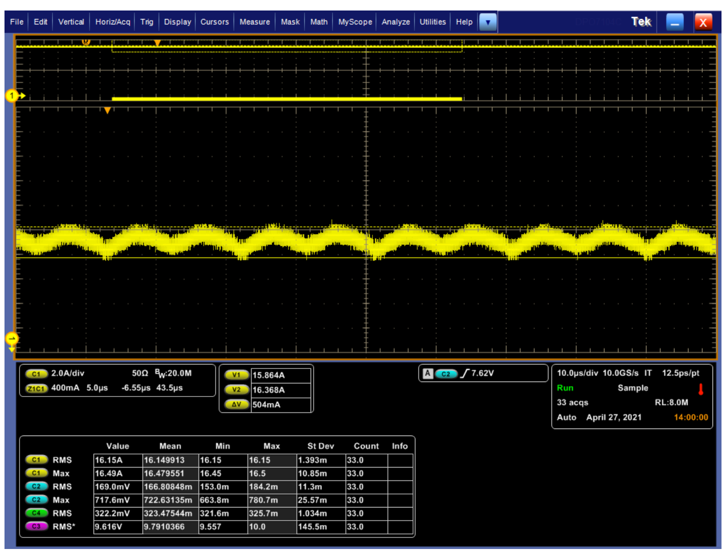

Figure 72: The output ripple current

-Channel 1(Yellow) : Output Current

4.4 Comparing of Toroidal and Integrated Transformers in Reliability Test

Thermal results were obtained at 24V@16A, 384W output power. The results were obtained at room temperature. Firstly, the thermal test was performed by using two pieces of EFD 5056 transformer at 105 kHz. The temperature of EFD5056 is around 83° in room conditions as shown in Fig.73.

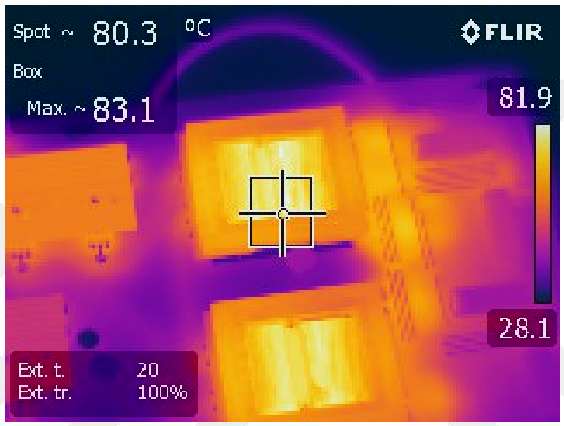

Figure 73: Thermal result for 2 pieces EFD5056 transformer

In EFD type transformers, the leakage inductance is deliberately put inside the transformer. The leakage inductance is used as a resonant inductance. The leakage inductance is the part where the energy is stored and the temperature is high on the area of leakage inductance.

The efficiency results are calculated for the power supply unit at 220VAC input voltage. The maximum efficiency is calculated as 93% for two pcs EFD 50/56 transformers. The efficiency versus graph is depicted in Fig.74.

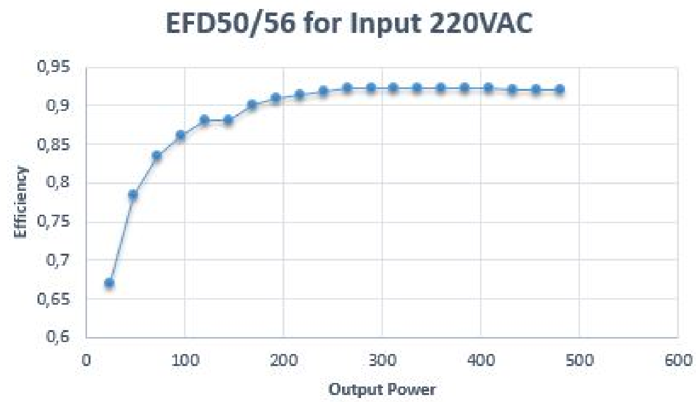

Figure 74: Efficiency graph of power card for EFD 5056 transformer at 220VAC

In the other test condition, one piece of 47/27/10 size toroidal transformer was used. ER3010 was used as the resonant coil. The toroidal transformer was measured in room conditions as shown in Fig.75. The maximum temperature is measured as 81°.

Figure 75: Thermal result for toroidal transformer

The air gap is distributed homogeneously on the toroidal transformer and therefore the temperature is evenly distributed over the whole surface of the transformer. The thermal results are shown in Tab.4.

Table 4: Thermal results for components of LLC resonant converter

	$2xEFD50/56$	$1xToroidal47/27/10$
Transformer	83°	81°
MOSFET	66°	66°
Resonant Coil	Integrated to the transformer	72°
Synchronous Rec.	72°	72°
Ambient	25°	25°

The efficiency has been calculated with various loads that are changed from 1A to 20A in 24Vdc. The maximum efficiency is calculated to be 94% for the power supply unit as shown in Fig.76.

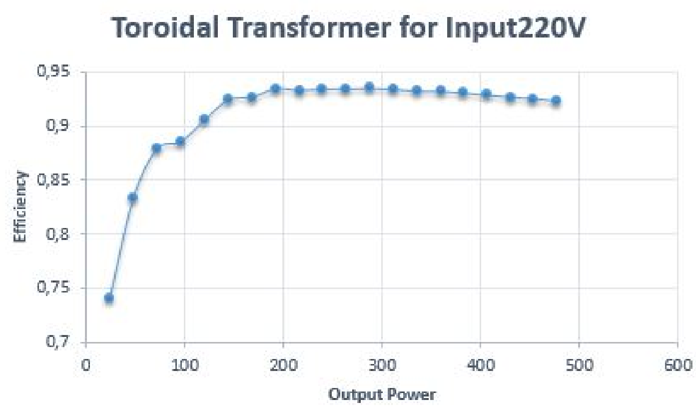

Figure 76: Efficiency graph of power card for toroidal transformer at 220VAC

CHAPTER V

CONCLUSIONS AND FUTURE WORK

5.1 Conclusions

In this thesis, power circuit design criteria, which is an important part of today's developing TV technologies, are emphasized. OLED TV does not have a backlight structure. Each pixel is controlled separately thanks to the RGB (Red Green Blue) LEDs in every pixel. Each pixel is individually powered and can create different lights. The supply voltage of OLED TVs is generally supplied in the range of 20-28V. The output voltage was designed to be a constant 24V output voltage in the thesis study.

This thesis has presented design and simulation results for the slim power card. The slim design represents that the maximum component height is 15mm. So, each component was selected according to this condition. The power card happens in 3 main stages which are the EMI stage, PFC stage and LLC resonant converter stage.

First of all, the PFC stage was designed interleaved to transfer more power and reduce the stress on the components. For the PFC stage, the input parameter is in the range of 100VAC- 265VAC and 50/60Hz. The input voltage is variable, the output voltage is constant and boosts to 390VDC. Its efficiency is around 95% at 100VAC. As the input voltage increases, the coil current is reduced and the losses decrease, so the efficiency can be up to 97%.

LLC driver is selected as FAN7631. The important parameters and equivalent circuits of the LLC resonant converter were briefly described. A 384W, 390Vdc input voltage, 24V@16A output parameters LLC resonant converter was designed with two type transformers which are toroidal and EFD type transformers. EFD type transformer is an integrated transformer. So, the most heated point of the transformer is the area of the leakage inductance. The leakage inductance is used as a resonant inductance in this type of transformer. For the toroidal transformer, the leakage inductance was obtained as small as possible. The external coil was used as resonant inductance. The toroidal transformer transfer more efficient than the integrated EFD type. Toroidal transformer has distrıbuted air gap, which provides homogenously distributed heat. The simulation results are verified with experimental results. The system waveforms are given for different load conditions. The maximum efficiency of the LLC resonant converter is measured to be 97%. At the 384W output power, the efficiency is calculated as 96%.

Temperature and total card efficiency measurements were taken using a toroidal transformer and EFD 50/56 transformer. Ae and core parameter values of these transformers are chosen to be close to each other. The maximum efficiency of the power supply is calculated as 93% by using 2 pcs EFD 50/56 integrated transformers. The temperature results were taken under room conditions, its maximum temperature is 83°. The leakage area of the transformer becomes generally hotter. By using a toroidal transformer, the maximum efficiency is calculated as 94%. The heat is distributed homogenously on the entire core surface and the maximum temperature was measured as 81°.

Core loss, eddy current, copper loss, hysteresis loss, and other losses occur on the transformer. When 2 pcs EFD50 / 56 are used, these losses increase even more. This has a negative effect on the transformer as temperature and efficiency. Using a toroidal transformer is more advantageous in terms of thermal. In terms of cost, toroidal transformers can be 2-3 times more expensive. Appropriate material selection should be made by considering cost and performance parameters in the design.

5.2 Future Work

Si MOSFET was chosen as the switching element. There are switching losses in the opening and closing interval of the MOSFETs that can not be controlled by the designer. With the development of technology, SIC or GAN MOSFET can be used instead of Si MOSFET. The switching losses can be reduced and higher efficiency can be obtained. Because on-time and off-time are smaller than Si MOSFET. Gallium nitride(GAN) MOSFET and silicon carbide(SIC) MOSFETs can operate at higher frequencies about 1MHz, 2MHz. Fuji LLC controller supports between 44-400 kHz frequency. NCP1631 interleaved PFC controller supports a maximum 240kHz. So, the controllers must be changed when SİC and GAN MOSFET will be used at high frequency. SİC and GAN MOSFET are 3-5 times more expensive than Si MOSFET. Additionally, the controller of SIC and GAN MOSFET is more expensive than low switching controllers. So, Si MOSFET was chosen for the thesis study. When the frequency is increased, the size of passive materials can be reduced. In this way, the same power can be transferred with a smaller field and higher efficiency.

In the future, GAN and SIC MOSFET can be used more widely with the decrease material cost. Si MOSFET was chosen as the switching element. There are switching losses in the opening and closing interval of the MOSFETs that can not be controlled by the designer. With the development of technology, SIC or GAN MOSFET can be used instead of Si MOSFET. The switching losses can be reduced and higher efficiency can be obtained. Because on-time and off-time are smaller than Si MOSFET. Gallium nitride(GAN) MOSFET and silicon carbide(SIC) MOSFETs can operate at higher frequencies about 1MHz, 2MHz. Fuji LLC controller supports between 44-400 kHz frequency. NCP1631 interleaved PFC controller supports a maximum 240kHz. So, the controllers must be changed when SİC and GAN MOSFET will be used at high frequency. SİC and GAN MOSFET are 3-5 times more expensive than Si MOSFET. Additionally, the controller of SIC and GAN MOSFET is more expensive than low

switching controllers. So, Si MOSFET was chosen for the thesis study. When the frequency is increased, the size of passive materials can be reduced. In this way, the same power can be transferred with a smaller field and higher efficiency. In the future, GAN and SIC MOSFET can be used more widely with the decrease material cost.

APPENDIX A

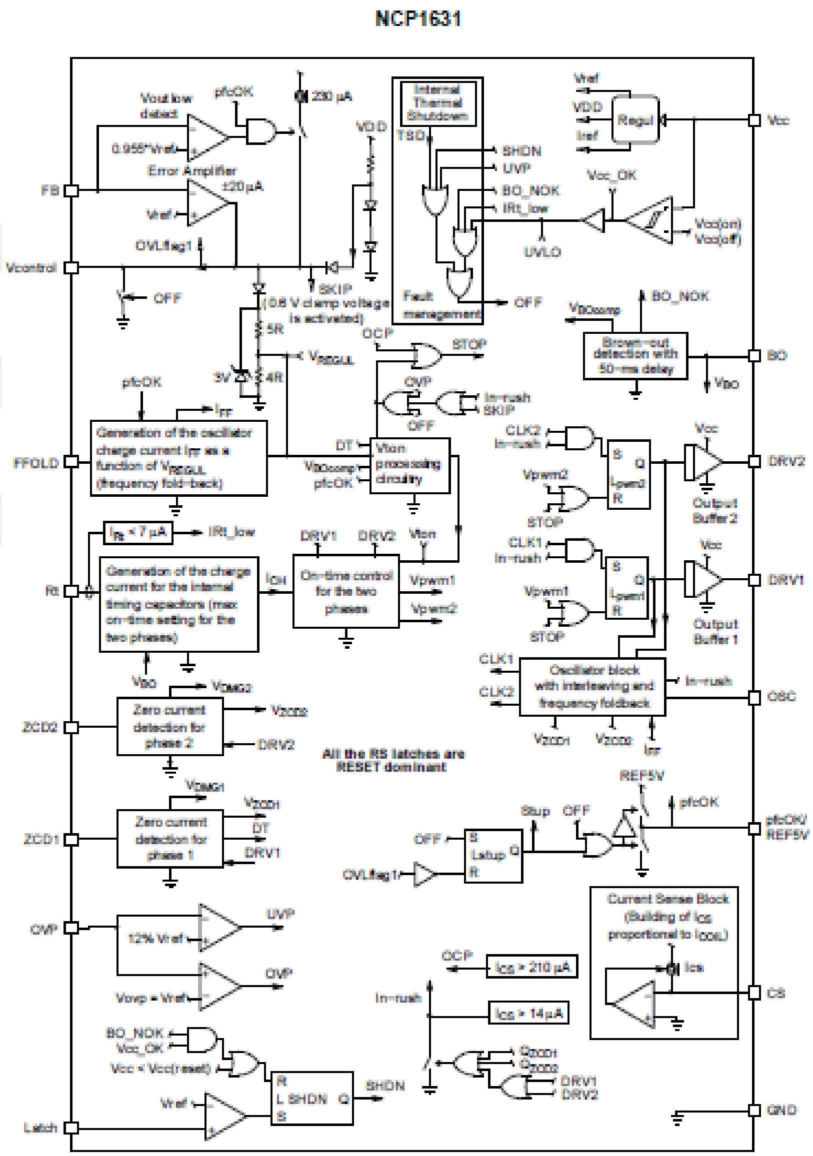

Figure 77: Functional block diagram of PFC controller [24]

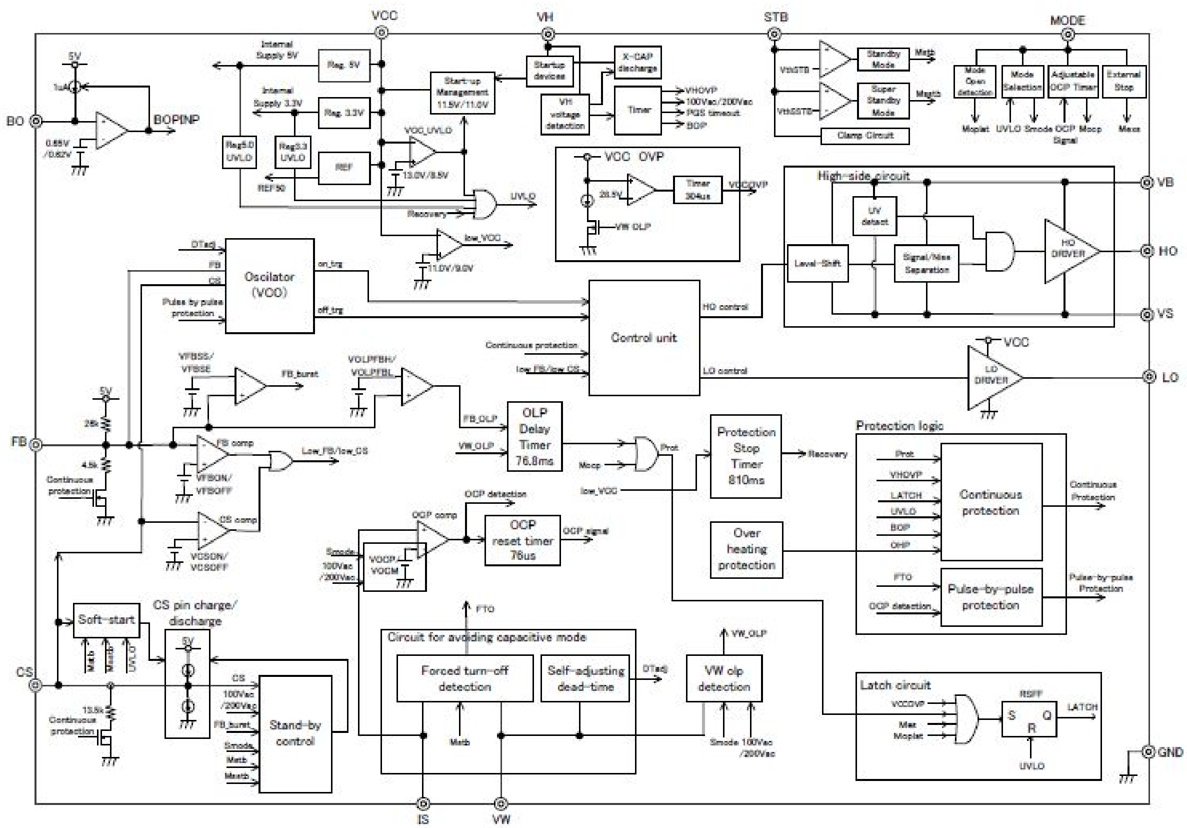

Figure 78: Block diagram of LLC resonant converter controller[31]

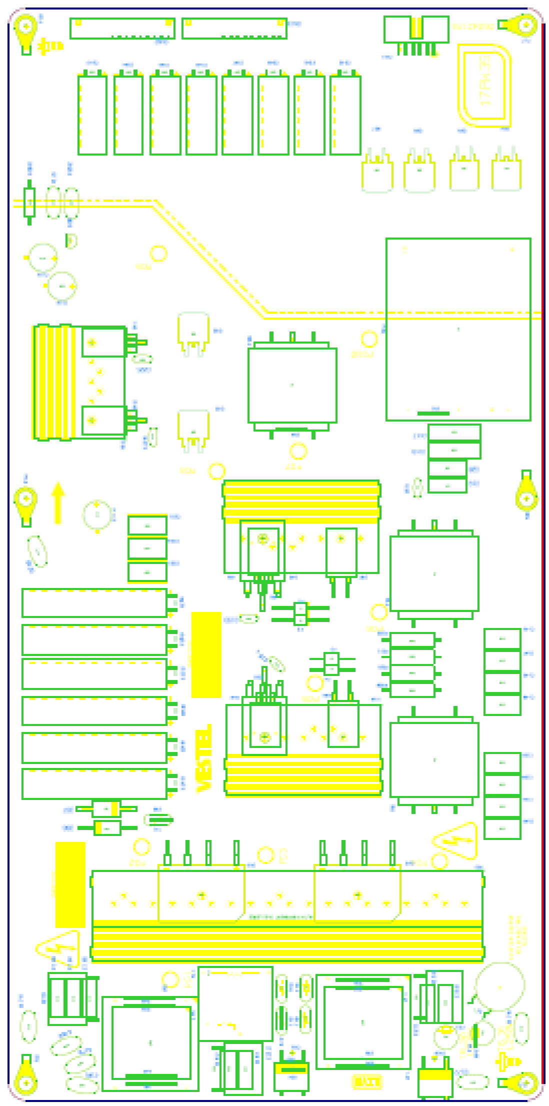

Figure 79: Layout design of the circuit for the upside

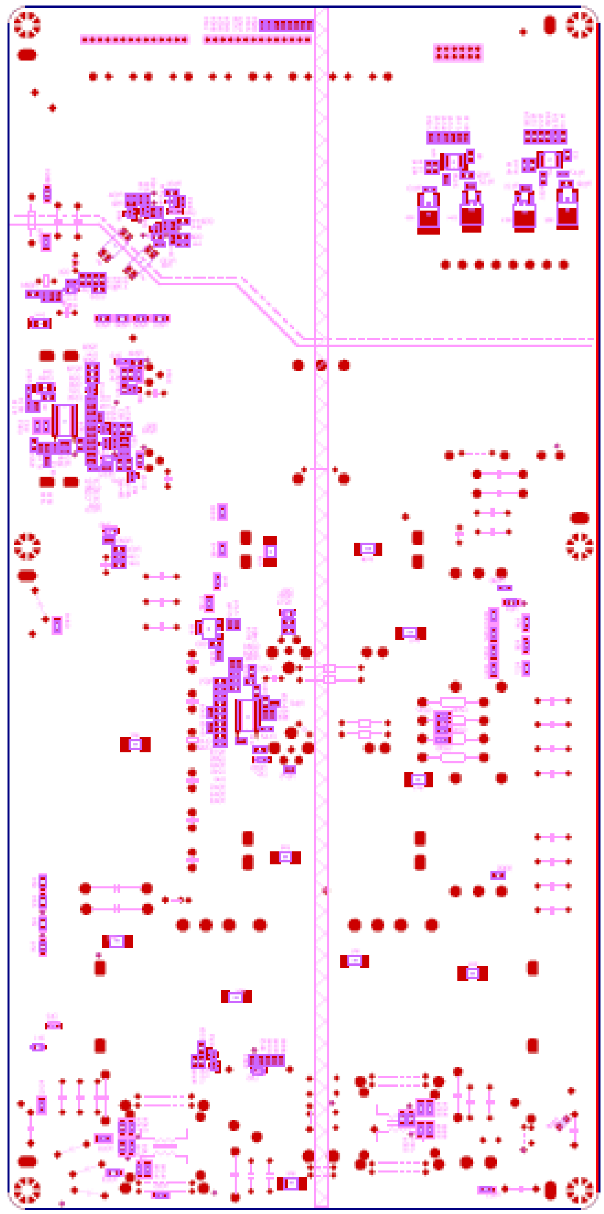

Figure 80: Layout design of the circuit for the downside

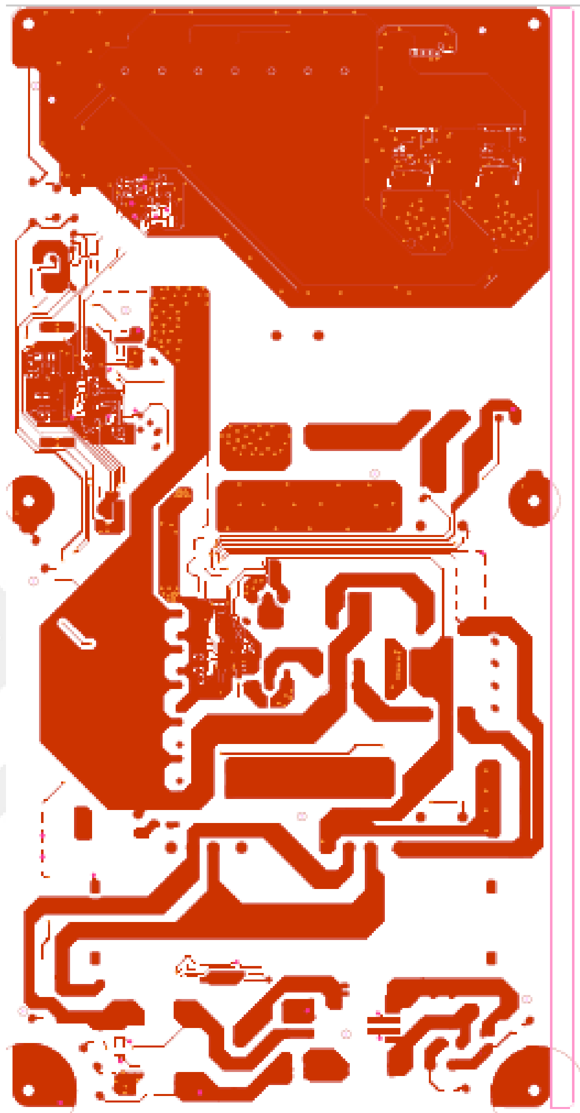

Figure 81: PCB paths for the downside

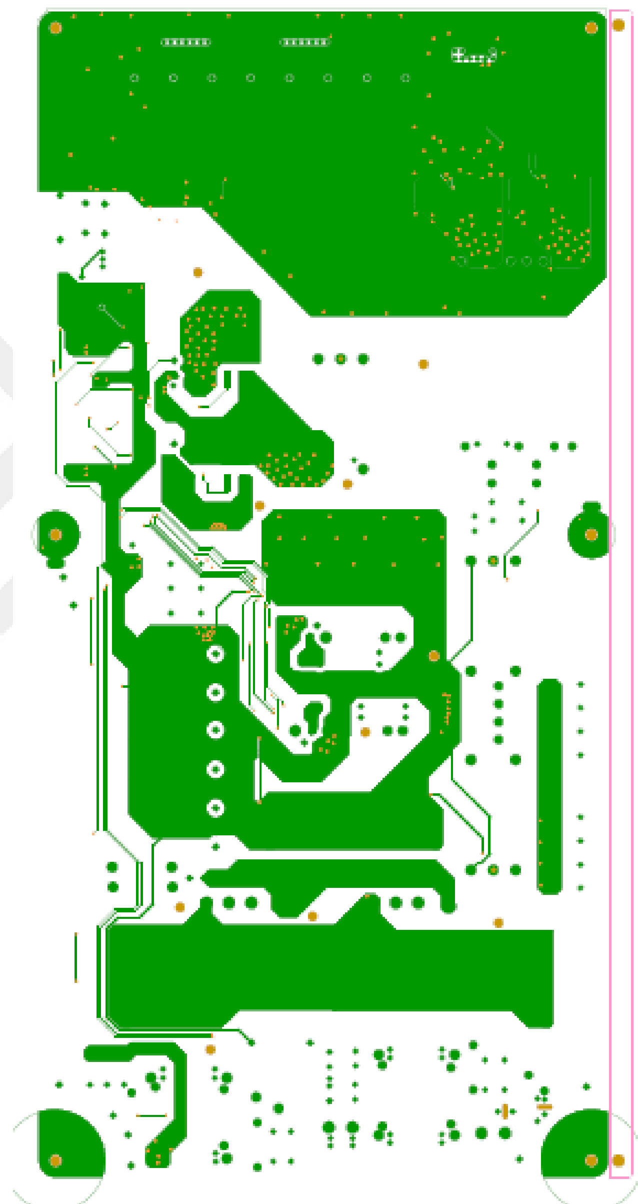

Figure 82: PCB paths for the upside

Figure 83: The topside of the PCB

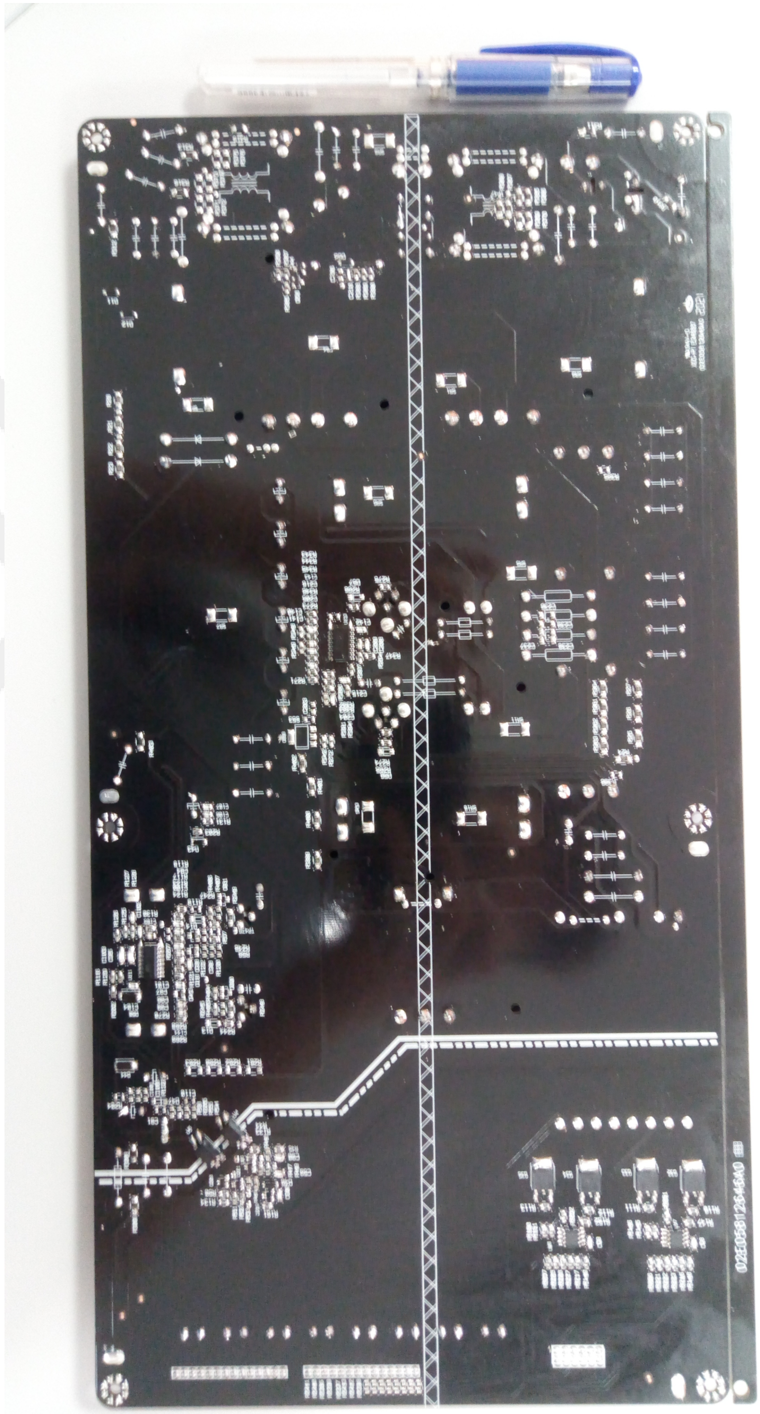

Figure 84: The bottom side of the PCB

Bibliography

[1] H. Murakami, "A 20-in color dc gas-discharge panel for tv display," *IEEE transactions on electron devices*, vol. 36, pp. 1–7, June, 1989.

[2] S.-C. Liao, "Optical response measurements of r/g/b mini-leds with short pulse voltage," *24th Microoptics Conference (MOC2019)*, pp. 274–275, Nov, 2019.

[3] Y. Yang, "High quantum yield colloidal semiconducting nanoplatelets and high color purity nanoplatelet qled," *IEEE transactions on nanotechnology*, vol. 18, pp. 220–225, 2019.

[4] S. Kunić, "Oled technology and displaysy," *54th International Symposium ELMAR*, pp. 31–35, Sep, 2012.

[5] P. R. W. Burns, "The first demonstration of television," *IET*, vol. 21, pp. 953–956, October, 1975.

[6] R. P. H. Adji, "Design of cathode ray tube analyzer rejuvenator for crt and cro," *IEEE*, 2015.

[7] A. Buttar, D. Jobling, and A. Rusznyak, "A high performance digital convergence and focus system for projection tv," *IEEE Transactions on Consumer Electronics*, vol. 38, pp. 734–740, August, 1992.

[8] J. K. Lim, H.-S. Tae, and D.-H. Lee, "New cost-effective driving circuit for plasma-tv," *IEEE*, 2009.

[9] M. İz, Tavman, and A. Turgut, "A study on cooling efficiency improvement of thin film transistor liquid crystal display (tft-lcd) modules," *13th Electronics Packaging Technology Conference*, pp. 536–541, 2011.

[10] S.-H. Lee, "Improvement of response time and contrast ratio in 42-inch tft-lcd panel for hdtv," *IEEE*, pp. 199–200, 2005.

[11] C.-Y. Han, "Fabrication of transparent full-colored quantum dot-light-emitting devices," *IEEE*, pp. 130–132, 2017.

[12] LG-Company, "Oled piksellerinin farkı nedir," tech. rep., LG Company, Korea, 2020.

[13] M. Rashid, *Power Electronics Handbooks*. Burlington, USA: Elsevier, 2011.

[14] L. Zhao, "A drive circuit of mosfet for ultrasonic power," *International Conference on Mechatronic Science*, pp. 1911–1914, August, 2011.

[15] Infeneon, "Coolmos™ sj mosfets benefits in hard and soft switching smps topologies," tech. rep., Infineon Technologies Austria, Austria, 2019.

[16] Würth, "Switch mode power supply topologies compared," tech. rep., Würth Electronics, Germany, 2021.

[17] I. P. Anders Lind, "Forward converter design note," tech. rep., Infineon Technologies, Austria, 2013.

[18] B. Yang, "Topology investigation for front end dc/dcpower conversion for distributed power system," *Virginia Polytechnic Institute and State University*, 2003.

[19] Bhaumik, "S. energy-efficient design and optimization of wireline access networks," *2011 Proceedings IEEE*, 2011.

[20] H. W. Chen, "Llc resonant current doubler converter," *A thesis submitted at the University of Canterbury*, DEC, 2012.

[21] H. Wan, "High efficiency dc-dc converter for ev battery charger using hybrid resonant and pwm technique," *Thesis, Virginia Polytechnic Institute and State University*, 2012.

[22] G. Yang, "Design of a high efficiency high power density dc/dc converter for low voltage power supply in electric and hybrid vehicles," *Phd thesis, Supulec, Paris-Saclay University*, 2014.

[23] Y. Ruiyang, "Design optimization of off-line power converters: from pwm to llc resonant converteres," *Thesis , Montpellier University*, 2012.

[24] O. Semiconductor, "Ncp1631 interleaved, 2-phase power factor controller," tech. rep., ON Semiconductor, USA, 2015.

[25] O. Semiconductor, "Power factor correction (pfc) handbook," tech. rep., ON Semiconductor, USA, 2014.

[26] O. Semiconductor, "Ncp1608 critical conduction mode pfc controller utilizing a transconductance error amplifier," tech. rep., ON Semiconductor, USA, 2015.

[27] D. Incorporated, "Zxgd3104ev2 user guide," tech. rep., Diodes Incorporated, USA, 2011.

[28] D. Incorporated, "Synchronous mosfet controller in so-8," tech. rep., Diodes Incorporated, USA, 2015.

[29] S. Microelectronics, "Simplified analysis and design of series-resonant llc half-bridge converters," tech. rep., MLD Group industrial power conversion division, Netherlands.

[30] S. Abdel-Rahman, "Coolmos^{TM} sj mosfets benefits in hard and soft switching smps topologies," tech. rep., Infineon Technologies North America(IFNA) Corp., USA, 2012.

[31] F. Electric, "Fa6a30/31n application note," tech. rep., Fuji Electric, Japan, 2015.

VITA

Samet Kurt graduated from Samsun Salıpazarı High School with the top honor in 2014. Then, he had a B.Sc degree of electrical and electronics engineering from Dokuz Eylul University in 2019. He has started his master of science at Özyeğin University in 2020. He joined the Power Electronics Design team at Vestel RD in august of 2019. He has worked currently as a hardware design engineer. He participated in different power electronics projects which are AC/DC and DC/DC converters for consumer electronics.

A.1 Publication

Samet Kurt, Gokturk Poyrazoglu, "Slim Design of LLC Resonant Converter for OLED TV by Using Toroidal Transformer", 2021 17-th International Conference on Electrical Machines, Drives and Power Systems ELMA2021,1 - 4 July 2021.